Constraints on ripple migration at Meridiani Planum from Opportunity and HiRISE observations of fresh craters

M. Golombek,[1] K. Robinson,[2] A. McEwen,[3] N. Bridges,[4] B. Ivanov,[5] L. Tornabene,[3] and R. Sullivan[6]

Received 16 April 2010; revised 19 July 2010; accepted 6 August 2010; published 18 November 2010.

[1] Observations of fresh impact craters by the Opportunity rover and in high-resolution orbital images constrain the latest phase of granule ripple migration at Meridiani Planum to have occurred between ~50 ka and ~200 ka. Opportunity explored the fresh Resolution crater cluster and Concepción crater that are superposed on and thus younger than the ripples. These fresh craters have small dark pebbles scattered across their surfaces, which are most likely fragments of the impactor, suggesting that the dark pebbles and cobbles observed by Opportunity at Meridiani Planum are a lag of impactor-derived material (either meteoritic or secondary impactors from elsewhere on Mars). Two larger, fresh-rayed craters in Meridiani Planum bracket ripple migration; secondaries from Ada crater are clearly superposed on and secondaries from an unnamed 0.84 km diameter crater have been modified and overprinted by the ripples. Three methods were used to estimate the age of these craters and thus when the latest phase of ripple migration occurred. The inactivity of the ripples over the past ~50 ka at Meridiani is also consistent with other evidence for the stability of the ripples, the lack of observed eolian bed forms in craters that formed in the past 20 years, and little evidence for much dune motion in the past 30 yr on Mars. Observations of crater morphology and their interaction with the ripples allow the development of a general time scale for craters in Meridiani Planum over the past million years.

Citation: Golombek, M., K. Robinson, A. McEwen, N. Bridges, B. Ivanov, L. Tornabene, and R. Sullivan (2010), Constraints on ripple migration at Meridiani Planum from Opportunity and HiRISE observations of fresh craters, *J. Geophys. Res.*, *115*, E00F08, doi:10.1029/2010JE003628.

1. Introduction

[2] The Mars Exploration Rover (MER) Opportunity landed in Meridiani Planum, a low-lying region of the heavily cratered highlands in the western hemisphere of Mars [*Golombek et al.*, 2003]. The region experienced extensive erosion and denudation in the Late Noachian [*Hynek and Phillips*, 2001; *Grant and Parker*, 2002], with valley networks that trend northwest, down the topographic gradient that was created by the flexure surrounding Tharsis [*Phillips et al.*, 2001; *Golombek and Phillips*, 2010]. The Opportunity rover landed on plains that are near the top of a broad section of hundreds of meters thick layered, sedimentary materials [*Arvidson et al.*, 2003; *Hynek*, 2004; *Edgett*, 2005; *Wiseman et al.*, 2010] that disconformably overlay the Noachian cratered terrain in this area [*Hynek et al.*, 2002; *Arvidson et al.*, 2003] but may be interbedded elsewhere [*Edgett*, 2005]. The layered rocks generally bury the valley networks in the cratered terrain, implying they are younger [*Hynek et al.*, 2002; *Hynek and Phillips*, 2008]. Measurement of the size-frequency distribution of a population of degraded craters >1 km in diameter shows that the layered materials are also Late Noachian to Early Hesperian in age [*Lane et al.*, 2003; *Arvidson et al.*, 2006; *Hynek and Phillips*, 2008], indicating that they were deposited after the period of denudation that stripped the region.

[3] The plains surface that Opportunity has explored is dominated by granule ripples composed mostly of a surface lag of 1–5 mm diameter hematite spherules (called blueberries) underlain by a poorly sorted mix of fine to very fine basaltic sand [*Soderblom et al.*, 2004; *Sullivan et al.*, 2005, 2007; *Weitz et al.*, 2006]. The hematite spherules are concretions that have been eroded out of the underlying weak layered sulfate-rich sedimentary rocks through abrasion by saltating sand [*Soderblom et al.*, 2004]. The sedimentary

[1]Jet Propulsion Laboratory, California Institute of Technology, Pasadena, California, USA.
[2]State University of New York at Binghamton, Binghamton, New York, USA.
[3]Lunar and Planetary Laboratory, University of Arizona, Tucson, Arizona, USA.
[4]Johns Hopkins University Applied Physics Laboratory, Laurel, Maryland, USA.
[5]Institute for Dynamics of Geospheres, RAS, Moscow, Russia.
[6]Department of Astronomy, Cornell University, Ithaca, New York, USA.

0148-0227/10/2010JE003628

rocks, known as the Burns formation have a composition and texture consistent with evaporitic sandstones that were likely deposited in acidic saline interdune playas [*Squyres et al.*, 2004a; *Grotzinger et al.*, 2005; *Clark et al.*, 2005]. Sediments were subsequently reworked by wind and in some locations surface water and later underwent extensive diagenesis (including formation of the hematite concretions) via interaction with groundwater of varying chemistry [*McLennan et al.*, 2005]. The blueberries are more resistant to erosion than the sulfate-rich bedrock, so once they erode out of the sedimentary rocks, they concentrate at the surface as a lag deposit.

[4] Eolian erosion of the weak sulfate bedrock is also revealed by a number of impact craters in varying stages of degradation that have been visited by Opportunity [*Golombek et al.*, 2006a]. The observed craters range from fresh and relatively unmodified, to highly eroded and infilled, and document progressive eolian erosion of the weak sulfate bedrock and infilling by basaltic sand [*Grant et al.*, 2006, 2008; *Golombek et al.*, 2006a]. Counts of these craters including those <250 m in diameter, which are clearly sparse in high-resolution orbital images, demonstrate that the average crater retention age of the basaltic sand and ripple surface is Late Amazonian [*Lane et al.*, 2003].

[5] Most of Opportunity's >20 km traverse has been over a surface dominated by granule ripples that have varied from small (cm size) and widely spaced (relative to their height) near the landing site to much larger (m sized) and more closely spaced to the south. The largest ripples are found in terrain with frequent pavement outcrop 3–4 km north and south of Victoria crater (excluding the smooth annulus surrounding Victoria). The largest and best developed ripples trend mostly north-south and appear older and more cohesive, than younger, cohesionless ripples that trend northeast-southwest [*Sullivan et al.*, 2005]. By analogy with granule ripples on Earth [*Bagnold*, 1941; *Sharp*, 1963; *Anderson*, 1987; *Anderson and Haff*, 1988; *Fryberger et al.*, 1992], the ripples in Meridiani migrate by reptation or creep of coarse grains on the surface from impact by saltating sand. Although granule ripples on the Earth have been referred to by a variety of names (e.g., ridges, megaripples and granule ripples [*Bagnold*, 1941; *Sharp*, 1963; *Sullivan et al.*, 2005, 2008; *Jerolmack et al.*, 2006], we will refer to them as granule ripples to emphasize the coarse surface particles [e.g., *Fryberger et al.*, 1992; *Zimbelman et al.*, 2009], even though most of the coarse surface fraction at Meridiani Planum is 1–2 mm and thus technically very coarse sand, rather than granules (2–4 mm). For simplicity in this paper, all use of the term "ripples" will refer to north trending "granule ripples" unless otherwise designated (e.g., the few examples of smaller, single grain size, ordinary ripples inside craters).

[6] Small craters observed by Opportunity document relatively rapid erosion and infilling by the basaltic sand [*Grant et al.*, 2006; *Golombek et al.*, 2006a]. Fresh small craters in sulfate sedimentary rock exhibit blocky interior walls and ejecta superposed on the ripples (e.g., Vega, Resolution, Concepción). Craters with shallower sandy interiors, some ejecta blocks that are planed off parallel to the ripple surface, and ripples that have merged with and/or partially cover their rims (e.g., Viking, Voyager, Fram, Kaikos) are likely older. Craters with blocky rims, most of their ejecta planed off along the sand surface, and shallower sandy interiors (e.g., Viking, Voyager) are even older. With more erosion and infilling, the craters become still shallower, ripples cover their rims and most of the ejecta and rim relief is planed off to the level of the ripples (e.g., Naturaliste, Geographe). Highly eroded craters have no ejecta, backwasted and eroded rims that are covered by ripples, and little exposure of sulfate bedrock (e.g., Eagle, Jason, Alvin). Finally, craters like Vostok, are almost completely filled in with sand and show nothing more than a circular rim of planed off sulfate blocks. This progression in degradational state shows that eolian activity has modified impact craters and that the level of erosion and infilling can be used as a proxy for the relative age of the crater, with some craters younger than the ripples and others older [*Grant et al.*, 2006; *Golombek et al.*, 2006a].

[7] In this paper, we constrain the age of the most recent phase of migration by the older north trending granule ripples that dominate the surface explored by Opportunity. We start by describing the Resolution crater cluster (section 2) and Concepción crater (section 3) explored by Opportunity that are younger than the north trending ripples. Next we describe two larger, fresh-rayed impact craters on Meridiani Planum that bracket the latest phase of ripple migration (section 4). We use three methods to constrain the age of migration of these ripples, with all three methods suggesting the north trending granule ripples were last active between ~50 and ~200 ka (section 5). Finally, these results are discussed in context with other work and observations consistent with this age, with older and younger craters that can be placed into a general time scale for crater modification on Meridiani Planum, and with other observations on Mars that show little evidence for recent dune migration, suggesting possible climates that might have been more capable of supporting migration of eolian bed forms prior to ~100 ka (section 6).

2. Resolution Crater Cluster

2.1. Opportunity Observations

[8] On sols 1818–1854 Opportunity explored a cluster of very fresh craters, informally named the Resolution crater cluster (after the first crater explored) about 2.3 km southwest of Victoria crater. The crater cluster was recognized in High Resolution Imaging Science Experiment (HiRISE) images prior to arrival and the rover path was planned to pass among them. The cluster consists of about 50 craters, of which the four largest are about 5 m in diameter (informally named Resolution, Adventure, Discovery and Granbee) that are scattered across a 120 by 80 m area. In the HiRISE images, the craters appear, based on their morphology, to be the freshest visited up to that time by the rover. The rims are continuous and appear unmodified by the ripples with ejecta blocks superposed on top of the ripples. Opportunity imaged three of the four largest craters up close, obtained a full Navigation Camera (Navcam) stereo panorama during a "drive by shooting" in the midst of the highest concentration of small (<1 m diameter) craters on sol 1852, and obtained selected Panoramic Camera (Pancam) color images. Craters observed in both HiRISE and rover images are shown in Figure 1 along with the rover traverse.

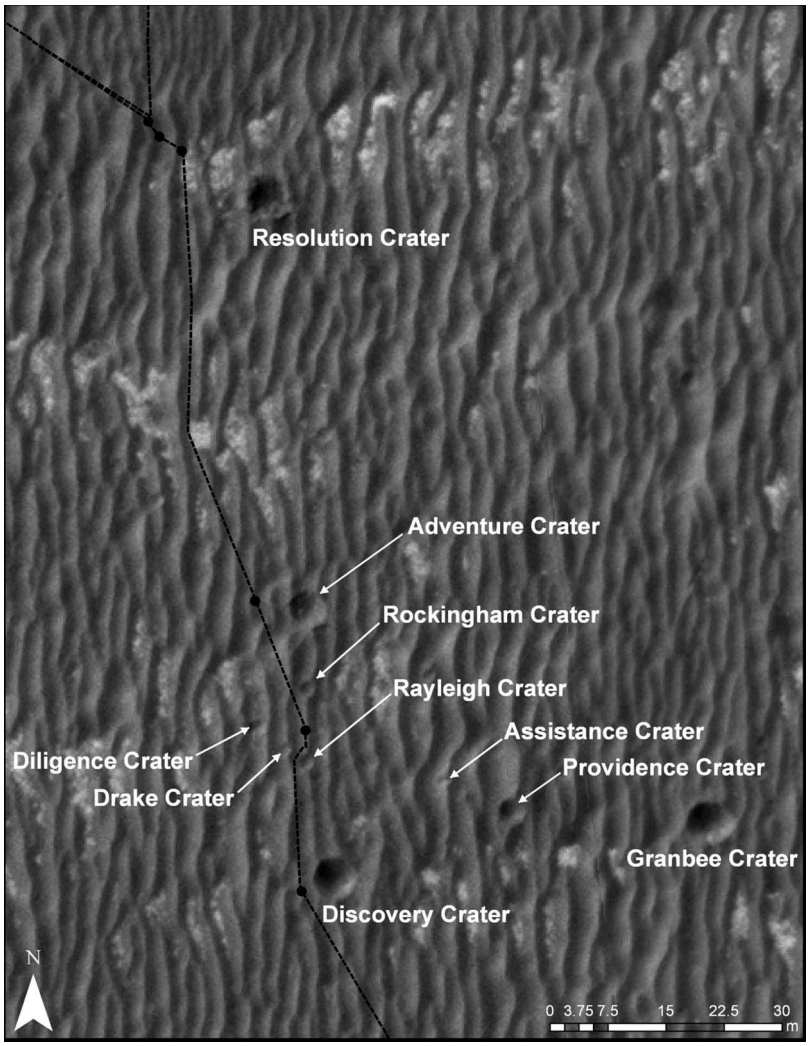

Figure 1. HiRISE image of the Resolution crater cluster showing crater names with path and imaging stops by the Opportunity rover. The four largest craters are 5–6 m in diameter. All craters appear fresh and unmodified by the north trending ripples, suggesting that they are younger than the latest phase of ripple migration. The rover spent sols 1825–1849 at the closest rover stop to Resolution crater, sol 1851 adjacent to Adventure crater (Resolution and Adventure craters are 50 m apart), sol 1852 amidst the largest concentration of small craters (nearest Rayleigh and Drake craters), and sol 1854 near Discovery crater. Portion of HiRISE image PSP_009141_1780; this image, like all HiRISE images, is at a resolution of about 0.25 m/pixel.

2.1.1. Resolution Crater

[9] The first crater visited by Opportunity was Resolution crater, the northernmost of the four largest craters in the cluster. Resolution is about 5.25 m across and is characterized by a blocky, elevated rim of sulfate sedimentary rock (Burns formation). The ejecta is superposed on the ripples and appears fresh and uneroded (Figure 2). Blocky ejecta also lies on top of the adjacent Burns formation that has been planed off parallel to the ripples, indicating that erosion of the Burns formation occurred well before the impact. The interior of the crater is a mixture of sand and sulfate blocks. Minimal eolian modification of the crater is observed, besides the sand in the interior. Based on these relations between the ejecta and ripples, Resolution crater is the youngest crater observed by Opportunity to this point in her traverse. Also observed scattered on top of the adjacent surface are dark pebbles, which based on their color are likely mafic (magnesium and iron rich) material unrelated to the Burns Formation. Figure 3 shows a portion of the northern rim of Resolution crater and a large number of dark, centimeter sized pebbles sitting on top of the rim. Because of the apparent youthfulness and the minimal eolian modification of the crater, the simplest explanation is that these pebbles are fragments of the impactor.

2.1.2. Adventure Crater

[10] The second crater visited by Opportunity in the cluster was Adventure crater, which is 5 m in diameter. Adventure crater is much less blocky than Resolution, with Burns formation making up a portion of the eastern interior wall and rim of the crater with scattered blocks elsewhere (Figure 4). The north, south and east rims of the crater are composed of sand and are elevated with respect to sur-

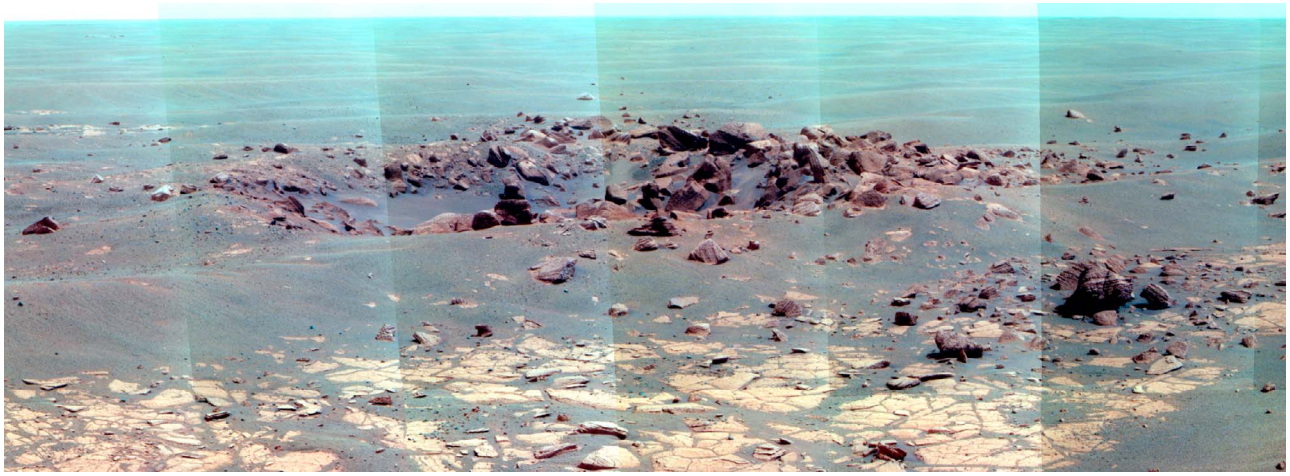

Figure 2. Pancam false color mosaic looking to the southeast of Resolution crater, which impacted into sulfate bedrock. The crater is fresh looking with a blocky rim and blocky ejecta that is superposed on the ripples. Sand appears in the interior of the crater, but the ejecta blocks do not appear heavily eroded. The crater is 5.25 m in diameter and 0.5 m deep.

rounding terrain. The north and south rims clearly truncate the north trending ripples, indicating the crater is younger. Eolian modification of the crater is minimal and limited to small, centimeter size secondary bed forms that are on the crater rim as well as the larger and older north trending granule ripples (Figures 4, 5, and 6).

2.1.3. Rockingham, Rayleigh, Drake, and Diligence Craters

[11] On sol 1852–1853, Opportunity stopped amidst the highest concentration of small craters within the cluster and imaged Rockingham, Rayleigh, Drake and Diligence craters from distances of less than 10 m with Navcam (and some targeted Pancam images). Rockingham, Rayleigh, and Drake craters are entirely in sand and are shown in Figures 5, 6, and 7). These three craters are about 2 m in diameter, clearly truncate and are superposed on the ripples and their crests, indicating they are all younger. Slightly steeper upper walls in Rockingham, lenticular layers exposed on the north wall of Rayleigh, and a pear shaped interior depression in Drake all suggest interior layering and/or different mechanical properties with depth. The layering exposed in Rayleigh (Figure 6) appears continuous with banding commonly exposed on the east side of the north trending ripple, suggesting that this banding is the surface expression of layers of material deposited during different phases of ripple growth. Craters too small to detect in HiRISE images (a few tens of centimeters or smaller) are also found nearby Rayleigh. Like the larger craters, eolian modification of these craters is minimal and limited to small, centimeter size secondary bed forms that are perpendicular to and superposed on the larger and older north trending granule ripples (Figures 4, 5, and 6). Diligence crater (1 m diameter) has a sandy interior depression, but appears to have also sampled bedrock with blocks of ejecta that are preferentially found to the north (Figure 8). Color Pancam images reveal dark centimeter size pebbles sitting on top of the northern rim,

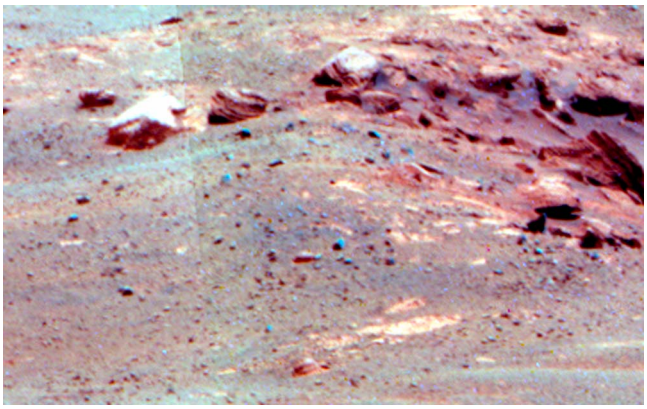

Figure 3. Detail of Pancam color mosaic of the northern rim of Resolution crater showing a large population of dark centimeter size pebbles. Because the crater formed after the ripples were active, these pebbles are probably fragments of the impactor.

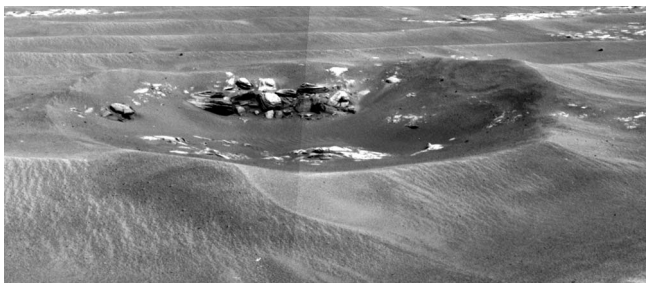

Figure 4. Navcam mosaic looking to the east-southeast of Adventure crater acquired on sol 1851. Crater has a blocky eastern interior wall but a sandy rim elsewhere, indicating the impactor excavated both sulfate outcrop as well as sandy ripples. Note the rim is both uplifted and clearly truncates north trending ripples, but that smaller centimeter size ripples perpendicular to the large ripples have formed. Adventure crater is about 5 m in diameter and 0.47 m deep.

Figure 5. Navcam mosaic looking north toward Rockingham crater with Adventure crater behind it acquired on sol 1852. Rockingham formed in the sandy ripple with a smaller crater in its north rim. Rockingham crater is 2 m diameter and 0.3 m deep. The smaller crater (K in Table 1) is 0.6 m in diameter and 0.1 m deep.

and adjacent sandy and bedrock surfaces (Figure 9), which are likely impactor fragments.

2.1.4. Discovery Crater

[12] The southernmost crater in the Resolution crater cluster visited by Opportunity is Discovery crater, which is just less than 6 m in diameter. It is almost entirely in sand, with small exposures of outcrop on the eastern rim and southwestern floor (Figure 10). The crater clearly truncates the ripples and preserves an uplifted rim. Color Pancam images show a population of dark pebbles dispersed across the southern rim (Figure 11) and a small patch of ordinary sand ripples on the crater floor (Figure 12). The only other eolian modification observed in these craters are small centimeter size secondary bed forms on their rim that are perpendicular and superposed on the larger and older north trending granule ripples. Three other craters, Assistance, Providence, and Granbee were imaged at a distance with Navcam from the rim of Discovery crater and all three appear superposed and younger than the ripples (Figures 13, 14, and 15). The observation that dark pebbles observed at

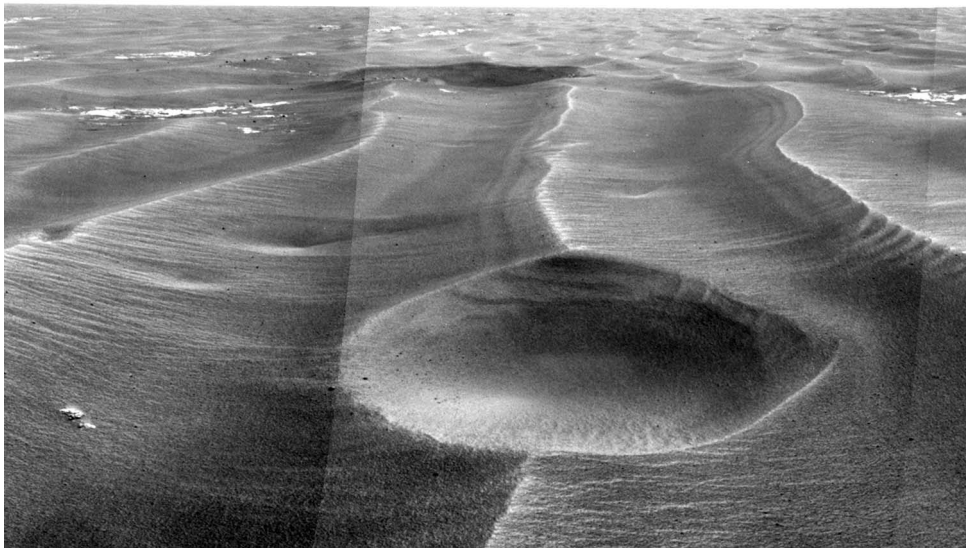

Figure 6. Navcam mosaic looking to the south of Rayleigh crater acquired on sol 1852, with Discovery crater in the background. Rayleigh crater exposes a cross section of the ripple to the south, showing that the banding on the east face of the ripple is made of layers that dip to the west. Steeper slopes suggest a stronger, cemented near-surface layer also exposed in trenches. Rayleigh crater is 2 m in diameter and 0.2 m deep. Note secondary ripples on the crater rim and ordinary ripples in the bottom of the crater. Smaller craters behind Rayleigh crater are from left to right: P, Q, R, S, and T in Table 1.

Figure 7. Navcam mosaic looking to the east of (left) Drake and (right) Diligence craters acquired on sol 1852. Drake crater is in sand, is superposed on a ripple, and has a pear-shaped interior depression. Diligence crater has blocky ejecta that are sitting on top of the ripples.

these fresh craters are likely fragments of the impactor, suggests that the dark pebbles and cobbles observed by Opportunity throughout her traverse on Meridiani Planum are a lag of impactor derived material that are either meteoritic (exogenic [*Schröder et al.*, 2008]) or from elsewhere on Mars (i.e., ejecta such as Bounce rock or Marquette Island [*Squyres et al.*, 2004b; *Mittlefehldt et al.*, 2010]).

2.1.5. Crater Morphometry

[13] All craters imaged in stereo Navcam images from Opportunity were measured using the Maestro mission planning and data display software [*Parker et al.*, 2010; *Powell et al.*, 2010] to characterize their morphometry. Specifically, crater depth and diameter were measured for 29 craters with diameters between 0.2 and 6 m within about 10 m of the rover (Table 1). Stereo ranging errors for Navcam images can be as little as 1% of the distance [*Maki et al.*, 2003], implying ideal uncertainties that vary from about 1 cm for measurements at a distance of 1 m, to 0.1 m for measurements at distances of 10 m. We also measured crater diameters in HiRISE images, for cases where rims could be discerned (generally craters larger than about 2 m diameter). These diameter measurements generally agreed to better than 10% with those derived from the Navcam images. Using the Navcam measurements of depth and diameter, we find a depth/diameter ratio of ~0.1 (Figure 16). This depth/diameter ratio is about half of that expected for fresh primary craters formed by hypervelocity impact on the Moon and Mars [*Pike*, 1977; *Melosh*, 1989], but matches the depth/diameter ratio (0.1) measured for secondary craters on the Moon [*Pike and Wilhelms*, 1978] and many small Martian craters suspected to be secondaries [*McEwen et al.*, 2005; *Golombek et al.*, 2006b]. Because crater clusters probably form by fragmentation of weak projectiles in the upper atmosphere (see section 2.2), the lower depth/diameter ratio could be due to a primary impactor that has been greatly slowed by atmospheric friction. However, impact experiments of clustered impacts show that the cratering efficiency of the fragments is greatly reduced, so this could be the cause of the lower depth/diameter ratio [e.g., *Schultz and Gault*, 1985]. Alternatively, the cluster could actually be a young cluster of secondary craters. Based on the similarity of the Resolution crater cluster to other young primary clusters (see section 2.2) and the multiple ways to explain the smaller depth/diameter ratio, we slightly prefer the interpretation that the Resolution craters represent a primary cluster (but both hypotheses are viable). The measured depth/diameters of other crater clusters of around 0.2 (expected for a hypervelocity impact [*Daubar and McEwen*, 2009]), suggests that some projectiles that fragment in the

Figure 8. Pancam false color mosaic of Diligence crater acquired prior to driving on sol 1854 showing blocky ejecta sitting on top of the ripples and sandy interior.

Figure 9. Detail of Pancam false color images of the northern rim of Diligence crater showing dark pebbles that are most likely fragments of the impactor. Portion of right two images in Figure 8.

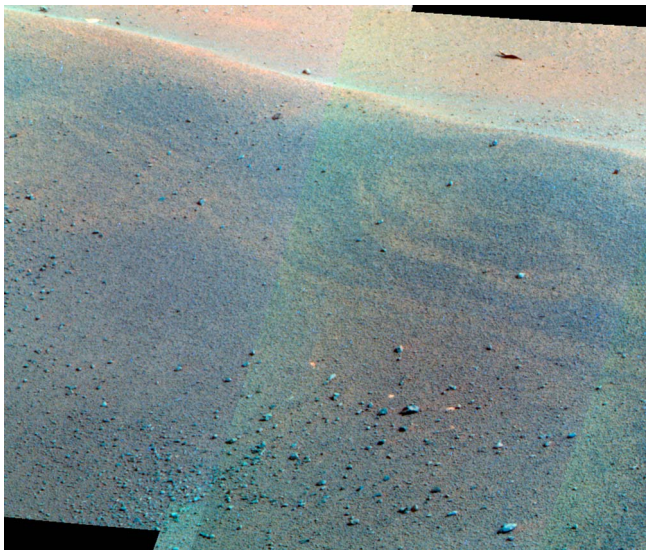

Figure 11. Pancam false color images of the southern rim of Discovery crater showing centimeter size dark pebbles that are likely fragments of the impactor. Images were acquired prior to driving on sol 1856.

atmosphere do not slow down much or lose their cratering efficiency.

2.2. HiRISE Observations of Fresh Primary Crater Clusters

[14] Craters associated with the Resolution cluster that were identified from the rover greater than 0.1 m diameter and in the HiRISE image are shown in Figure 17. Many of these are too small to be identified independently in the HiRISE images, but their locations are shown. Craters in the cluster fit within an ellipse that is about 140 m long by 100 m wide (oriented about N16°W) with 2 of the largest craters toward the south. This distribution is qualitatively "in family" with a class of craters that have impacted in the past 10 yrs found from repeat orbiter imaging [*Malin et al.*, 2006; *Daubar et al.*, 2010]. About 100 pristine craters have been discovered mostly in dusty areas initially imaged by Mars Orbiter Camera (MOC) on Mars Global Surveyor (MGS) or Context Camera (CTX) on Mars Reconnaissance Orbiter (MRO) and then reimaged by MOC, CTX and HiRISE. About 40% of these new impact sites are composed of clusters of craters typically spread across several hundred meters.

[15] Modeling by *Ivanov et al.* [2008, 2009] shows that these clusters form by fragmentation of weak impactors in the atmosphere and that the dispersion of the cluster is related to the density and strength of the impactor. Some of these clusters have one relatively large crater and a few smaller craters, whereas others consist of a number of small craters. Many consist of dispersed large and small craters similar to the Resolution cluster explored by Opportunity. Modeling shows that the largest craters are typically farther downrange as the largest fragment with the least atmospheric deceleration would be expected to travel the farthest. Two of the four largest craters at the southern edge of the

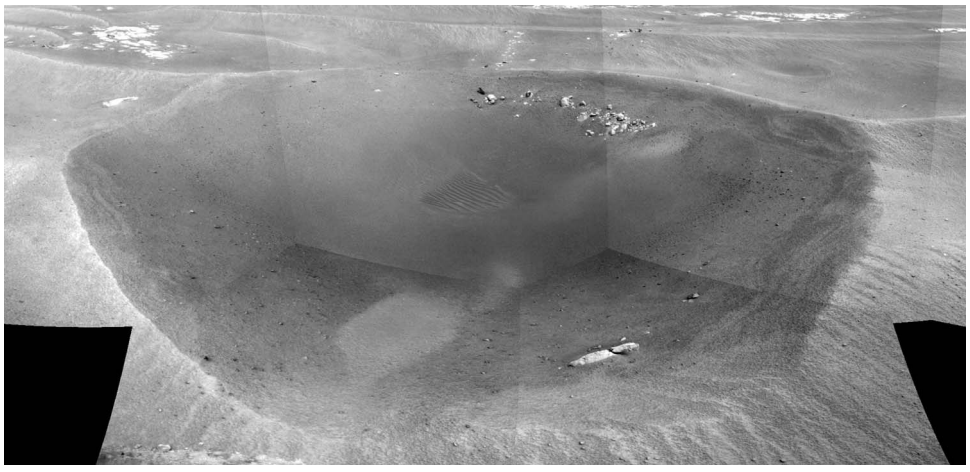

Figure 10. Navcam mosaic looking to the east of Discovery crater acquired on sol 1854. Note uplifted crater rim, with secondary ripples, that truncates large north trending ripples. Discovery crater is 5.5 m in diameter and about 0.6 m deep.

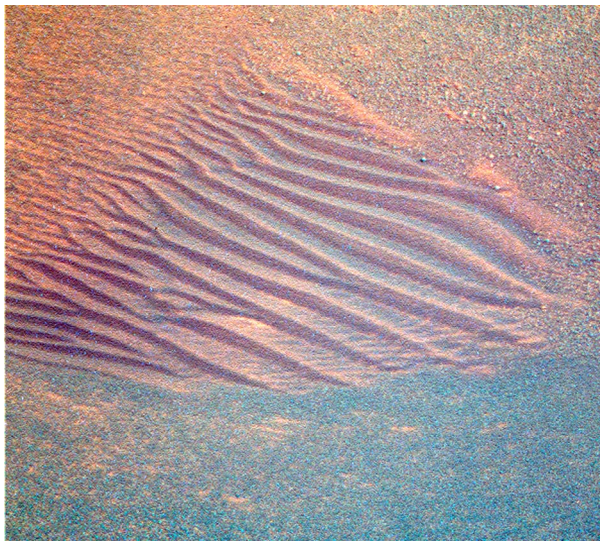

Figure 12. Pancam color image of ordinary sand ripples on the bottom of Discovery crater, which accumulated after the crater formed. Image was acquired prior to driving on sol 1856 and is about 0.8 m across.

Resolution cluster suggest that the impactor that formed this cluster, if it formed from a fragmenting primary, came into the atmosphere from the north and fell toward the south. Analysis of the Resolution crater cluster size-frequency distribution is similar to type 2 or 3 events in which a cascade of fragmentation events occurs for impactors with density 1.8–3 g/cm^3 [*Ivanov et al.*, 2008] and preliminary analysis of the dispersion of Resolution craters suggests that the impactor had a density of ~2 g/cm^3. This analysis also shows that the dispersion of the Resolution crater cluster is similar to that of other crater clusters that have formed in the past 10 years via fragmentation of exogenic impactors.

3. Concepción Crater

[16] Concepción crater is a 10 m diameter fresh crater with dark rays about 6 km south-southwest of Victoria crater that was explored on sols 2136–2176 of Opportunity's mission. In the red filter of HiRISE image ESP_012820_1780, Concepción's rim appears to truncate the north trending ripples, blocky ejecta (at about the limit of resolution) is present, and dark rays extend several crater radii to the southeast, and south that appear superposed on the ripples (Figure 18). These relations and comparisons with other craters, suggest that Concepción is the freshest and youngest crater visited by either rover.

[17] Opportunity imaged the interior of Concepción crater with Navcam and Pancam, partially circumnavigated the crater from the north clockwise to the southwest, and imaged the ejecta from multiple vantage points along this traverse. From the ground (Figure 19), Concepción crater is superposed on the large granule ripples, has a fresh blocky interior wall, uplifted rim, and ejecta and rays that lie on top of the ripples. The dark rays in the HiRISE image are composed of blocky ejecta of Burns Formation, indicating that the dark tone of the rays in the HiRISE image is due to shadows and shading produced by the ejecta blocks at the

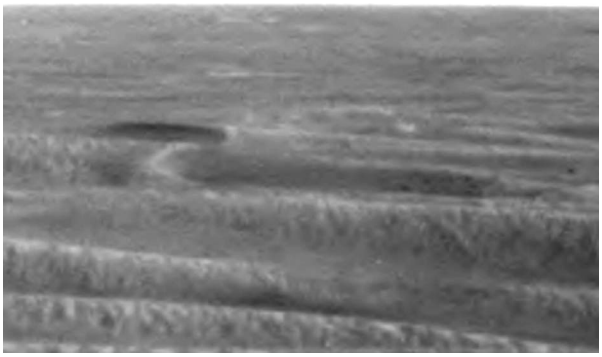

Figure 14. Navcam image looking to the east-northeast of Providence crater, about 27 m away. The crater truncates the ripples and excavated outcrop as indicated by ejecta blocks on top of ripples. Providence crater is about 4 m in diameter. This image was acquired after the drive on sol 1854 and is the highest-resolution image of this crater from the surface.

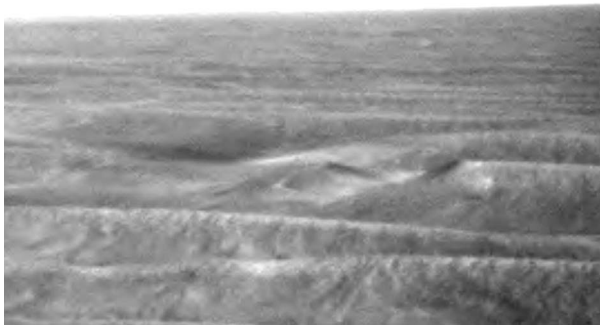

Figure 13. Navcam image looking to the northeast of Assistance crater, about 22 m away. The crater clearly truncates the ripple, indicating that it impacted after the latest phase of ripple migration. Assistance crater is about 1.5 m in diameter. This image was acquired after the drive on sol 1854 and is the highest-resolution image of this crater from the surface.

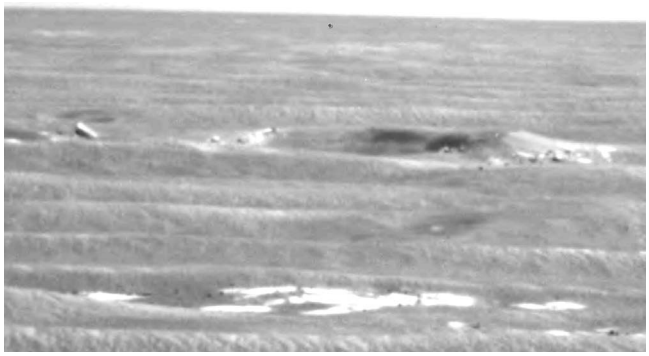

Figure 15. Navcam image looking to the east of Granbee crater, about 50 m away. Granbee crater excavated outcrop and deposited ejecta blocks on top of the ripples, indicating it impacted after the latest phase of ripple migration. Granbee crater is about 5.9 m in diameter. This image was acquired after the drive on sol 1854 and is the highest-resolution image of this crater from the surface.

Table 1. Resolution Cluster Crater Measurements in Meters[a]

Crater ID	HiRISE Diameter	Opportunity Diameter	Depth
D		0.25	
C		~0.2	
B		0.32	0.04
A		0.56	0.035
Res	5.55	5.25	0.475
3	1.85		
Adv	4.9	5.05	0.47
E		0.78	~0.10
ψ		0.15	
F		0.61	~0.06
G		0.85	~0.07
H		0.09	
I		~0.85	0.07
J		~0.2	~0.02
Rk	1.85	2	0.24
K		~0.6	~0.08
6	1.95[b]		
L	1.45	1.6	
M		0.75	0.08
N		0.45	~0.06
Dil	2.85	2.35	~0.25
Z (3)		~0.15	
Y		0.25	~0.02
X		~1.0	~0.11
W (3)		~0.4	
U		~0.4	
Dr	1.75	1.7	0.19
V		0.2	0.03
Ra	1.8	2.05	0.02
Q		~0.32	~0.03
R		~0.85	~0.1
P		~0.39	0.04
S		~0.8	~0.07
T		~0.45	~0.07
12	2.2		
O		~0.25	~0.03
As	1.2[b]	~1.75	~0.16
13	1.75		
Prov	3.9		
15	2.55		
16	1.8		
17	2.05		
Gran	5.75[b]		
β		0.25	
Dis	5.8	5.45	~0.61
π		0.2	
α		1.65	0.21
δ		0.11	
σ		~0.4	
λ		0.35	
φ		~0.2	
θ		0.45	
ε		0.4	
ζ		1.2	0.15

[a]Crater ID and locations shown in Figure 17. Approximate values (~) are less certain measurement.
[b]Trouble visualizing border.

relatively low 36° sun angle of the image. Because Opportunity has seen no dark outcrop anywhere along her traverse, the dark rays observed around other fresh craters in Meridiani (i.e., the fresh cluster described in section 6.4.2) also are likely produced by rays of blocky ejecta casting shadows.

[18] Even though Concepción appears to be the freshest crater visited by either rover, it still shows some eolian modification. First, the crater floor is predominantly sand confirming that sand continues to be mobilized in the current era at Meridiani Planum, and some of it has accumulated in Concepción's interior (Figure 19). If Concepción is a primary crater, its 1 m depth (rim to floor) is about half that expected, suggesting that the crater has been filled with about 1 m of sand. If Concepción is a shallow primary or secondary crater, much less sand could be in its interior. Second, drifts of sand have accumulated between ejecta blocks, in areas partly protected from the wind where the rate of sand migration should be less (Figure 20). Finally, many of the ejecta blocks appear etched, sculpted, and partially eroded by wind-driven sand (Figure 20). So even though migration of the larger, plains-covering, granule ripples is argued to be old herein, very fine sand has continued to be mobilized to the present day, even forming much smaller single-grain size ripples where this sand has accumulated in localized deposits (e.g., floors of Eagle, Discovery, and Concepción craters). The implication is that, since the time of Concepción's impact, the active, very fine sand has been too sparsely distributed to provide sufficient flux to drive the granule ripples significantly from their relatively ancient positions and configurations. However, the very fine sand flux has, during this same period, been sufficient to erode blocks of relatively weak Burns formation perched on the surface exposed to the saltating sand. This scenario is in agreement with observations of recently active ripples of very fine sand on the floor of Eagle crater aligned with that crater's transient wind streak [*Sullivan et al.*, 2005; *Jerolmack et al.*, 2006], very fine sand observed to be migrating from Victoria crater and filling old rover

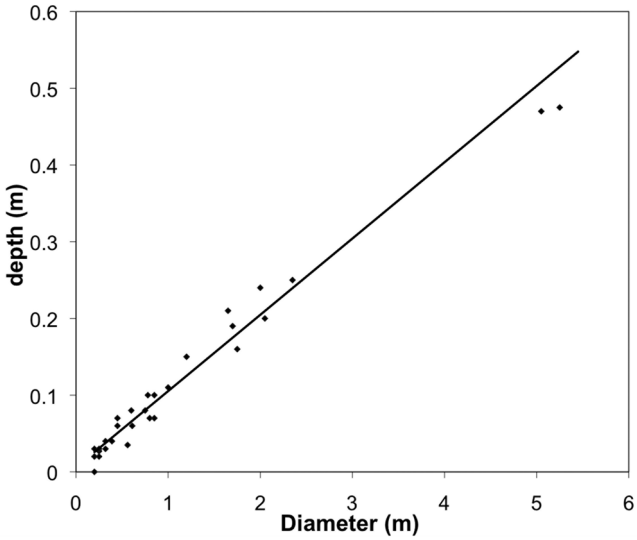

Figure 16. Plot of depth (d) versus diameter (D) for craters of the Resolution cluster for which crater depth could be measured from Navcam stereo images. Least squares linear regression best fit equation d = 0.0994 D + 0.0058 (not constrained to go through the origin) for 29 craters with a correlation coefficient of 0.99. The depth/diameter ratio of 0.1 is consistent with the craters being secondaries or primaries with reduced cratering efficiency due to fragmentation or that have been significantly slowed by the atmosphere. The similarity of the dispersion of craters in the cluster to other primary clusters that have formed in the past 10 years suggests the latter explanation. Depth, diameter data is in Table 1.

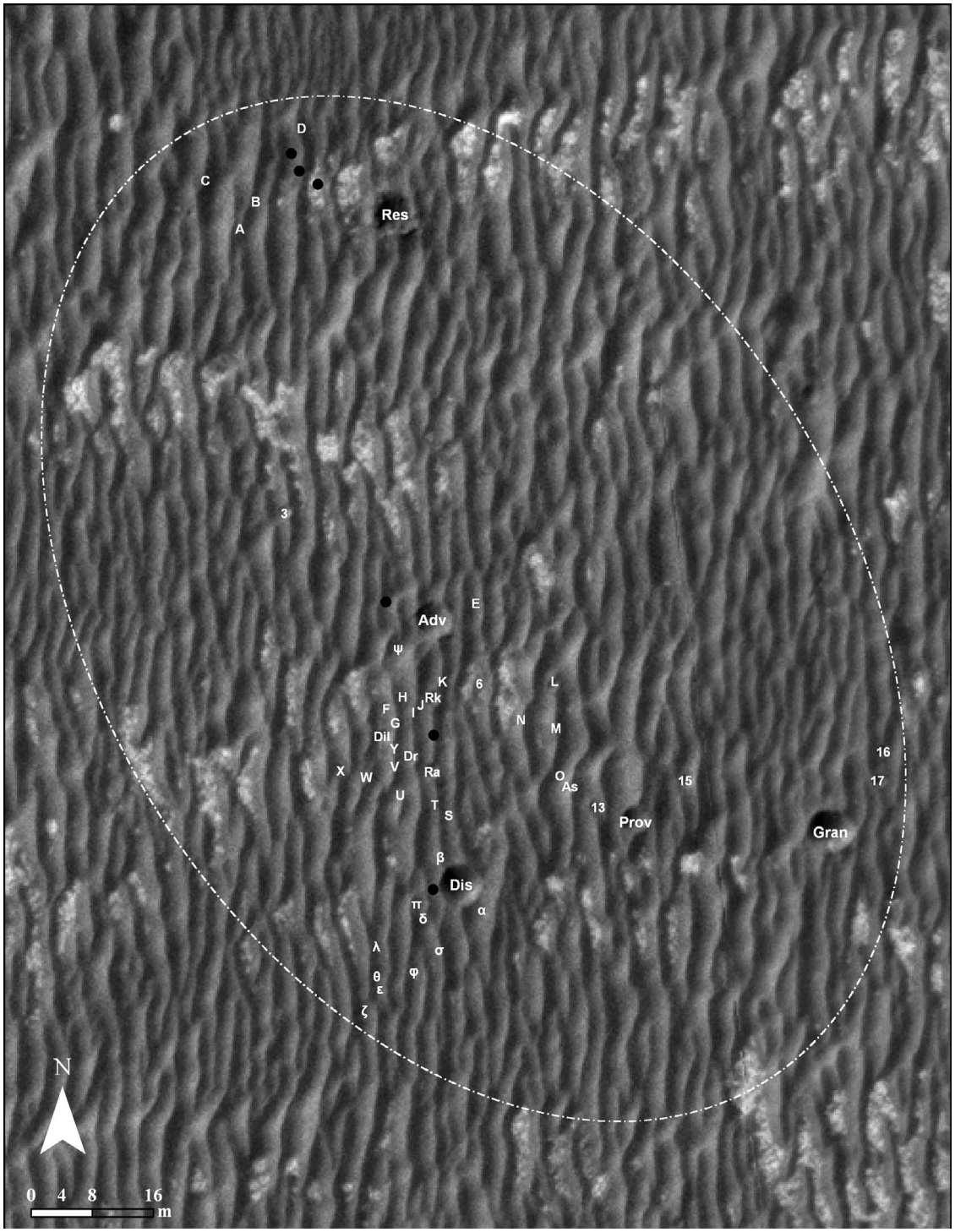

Figure 17. Portion of HiRISE image PSP_009141_1780 with craters of the Resolution cluster identified (data in Table 1), imaging stops of the Opportunity rover (black dots), and an example dispersion ellipse 141 m × 97 m, major and minor axes, respectively, at an azimuth of 344° measured clockwise. The two largest craters to the south suggest that the impactor fell from the north-northwest toward the south-southeast. Analysis of the size-frequency distribution of the craters and their dispersion suggests an impactor density of around 2 g/cm^3. The rover spent sols 1825–1849 at the northernmost rover stop closest to Resolution crater (Res), sol 1851 adjacent to Adventure (Adv) crater, sol 1852 amidst the largest concentration of small craters, Rayleigh (Ra), Drake (Dr), Diligence (Dil), Rockingham (Rk) craters, and sol 1854 at the southernmost rover stop near Discovery (Dis) crater, from which Providence (Prov) and Granbee (Gran) craters were imaged.

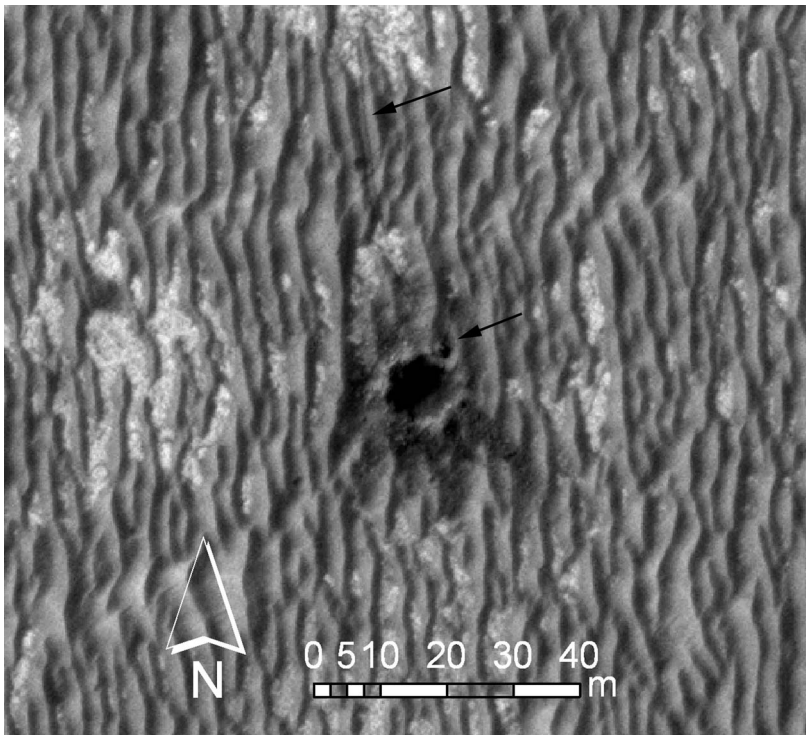

Figure 18. HiRISE image ESP_016644_1780 of Concepción crater showing blocky rim and ejecta and dark rays, the best defined extending to the southeast from the crater. The crater clearly truncates the ripples and the presence of rays suggests that this is the youngest crater visited by either rover. Opportunity is perched on the northeast rim (note shadow cast to the southeast — bottom arrow) and the rover tracks are visible from the north (top arrow).

tracks [*Geissler et al.*, 2008; 2010], and forming younger cuspate and secondary ripples from winds funneled along the troughs [*Sullivan et al.*, 2007]. In addition to the ongoing surface flux of sand since Concepción's impact, the impact itself likely liberated a local supply of very fine sand by disturbing the protective, slightly cohesive, lag of hematite spherules.

[19] Dark, centimeter sized pebbles are strewn across the surface around Concepción crater and its ejecta (Figure 21), as observed at the Resolution crater cluster as well as other fresh impact craters visited by Opportunity. The pebbles typically are perched on the surface and their dark color suggests that they are likely mafic (or iron rich) [e.g., *Schröder et al.*, 2008] material unrelated to the Burns

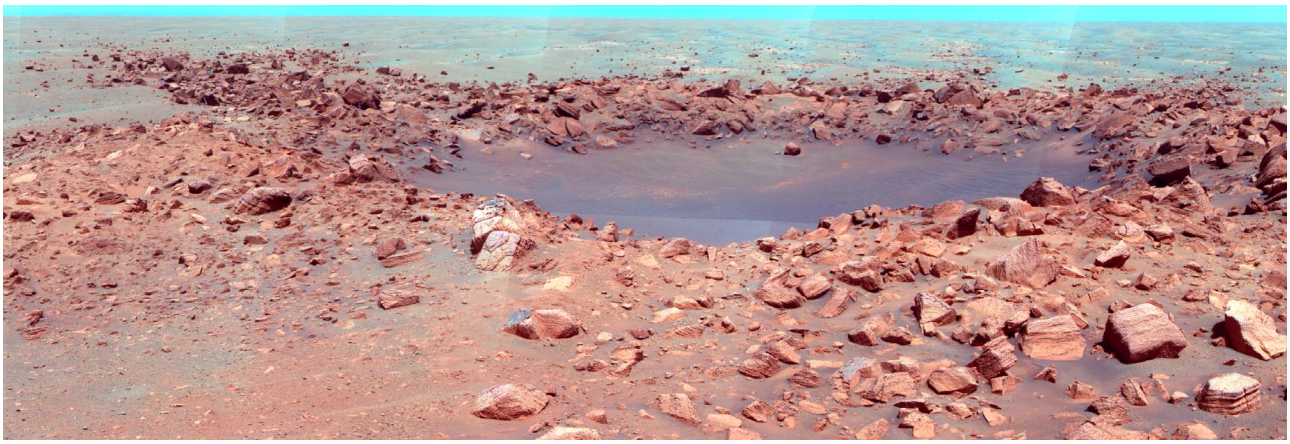

Figure 19. Pancam false color mosaic looking toward the south of Concepción crater acquired on sols 2139–2141 when Opportunity was about 5 m from the north rim. Ejecta of sulfate bedrock is scattered across the surface and in a blocky ray extending to the southeast and is clearly younger than the ripples. The dark ray observed in the HiRISE image (Figure 18) is produced by the shadows and shading from the blocky ejecta in the low Sun image (Sun angle is 36°). The interior of the crater is covered in dark sand, and dark sand is also filling in among the ejecta blocks in the bottom right of the mosaic.

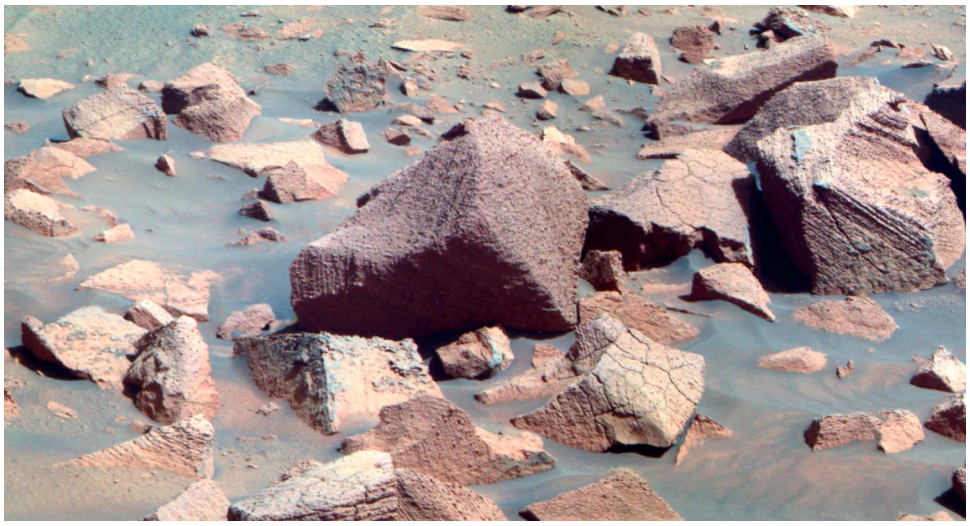

Figure 20. Pancam color image of fresh, dark sand filling among blocks of ejecta of Concepción crater. Note also etching of layers in some of the blocks, the abundance of blueberries in the rocks, and the lack of blueberries on the soil. The etching of the layers is likely due to eolian abrasion by saltating sand since the impact exposed the blocks. The lack of blueberries on the soil is either due to their being dispersed by the impact and/or having been covered up by the sand. Dark coatings are seen on several of the blocks. Image (about 1.4 m wide) acquired on sol 2166 looking to the southwest at the southeast crater ray, when Opportunity was about 10 m southeast of the Concepción crater rim.

Formation. Because of the youthfulness and the minimal eolian modification of the crater, the simplest explanation is that these pebbles are fragments of the impactor that formed the crater.

[20] Color Pancam images of the surface near the rover show a dearth of blueberry hematite spherules sitting on top of the surface (perched) adjacent to the crater or its ejecta (Figures 22 and 23). In particular most pavement outcrop surfaces have been swept clear of blueberries (e.g., Figure 21). The lack of blueberries on the surface seems incongruous with the ejecta bocks having many blueberries in the process of being weathered out, expressed as resistant spheres, exposed at the surface of the sulfate rock (e.g., Figure 24). In some cases, the blueberries released from the rock could be covered up by drifts of fine sand (e.g., Figure 20). However, in other cases the blueberries appear partially embedded or buried in a slightly cemented surface layer (e.g., Figure 23). In either case, the blueberries that typically sit perched on the surface are not found, suggesting that they have been buried or dispersed by the impact and its ejecta in agreement with the lack of hematite signature around larger, fresh-rayed craters in Meridiani (see section 6.3).

[21] In summary, comparing the morphology, degree of eolian modification, and the presence of rays at Concepción crater with the Resolution crater cluster, suggests that the Concepción impact is the younger of the two. Both Concepción and the Resolution crater cluster are younger than the latest phase of granule ripple migration at Meridiani Planum.

4. Larger, Fresh-Rayed Craters in Meridiani

4.1. Ada Crater

[22] Ada crater is one of two larger, fresh-rayed craters in Meridiani Planum that have impacted into surfaces similar to those traversed by the Opportunity rover (Figure 25). Ada is a 2.2 km diameter fresh-rayed crater located about 150 km east-southeast of Victoria crater. Ada ejecta and radiating rays appear bright in nighttime Thermal Emission Imaging System (THEMIS) thermal images suggesting that they have

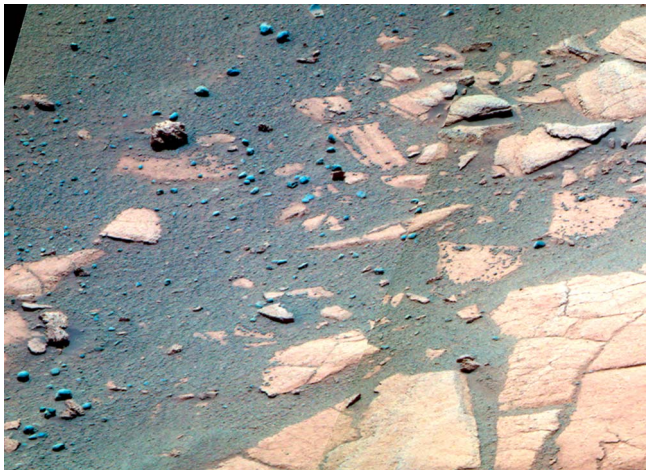

Figure 21. Pancam color image of the surface near Concepción crater showing numerous dark pebbles strewn across the surface. Pebbles are perched, and their dark color suggests that they are mafic (or metallic) fragments. The concentration of such dark pebbles around fresh impact craters suggests that the population of dark pebbles at Meridiani Planum are a lag of impactor-derived fragments. Note how blueberries appear embedded and/or cemented into the soil and how the outcrop has been swept free of blueberries. Pancam color image acquired on sol 2137, when the rover was about 16 m north of the rim of Concepción. Image is about 0.5 m across and pebbles are 1–2 cm in size.

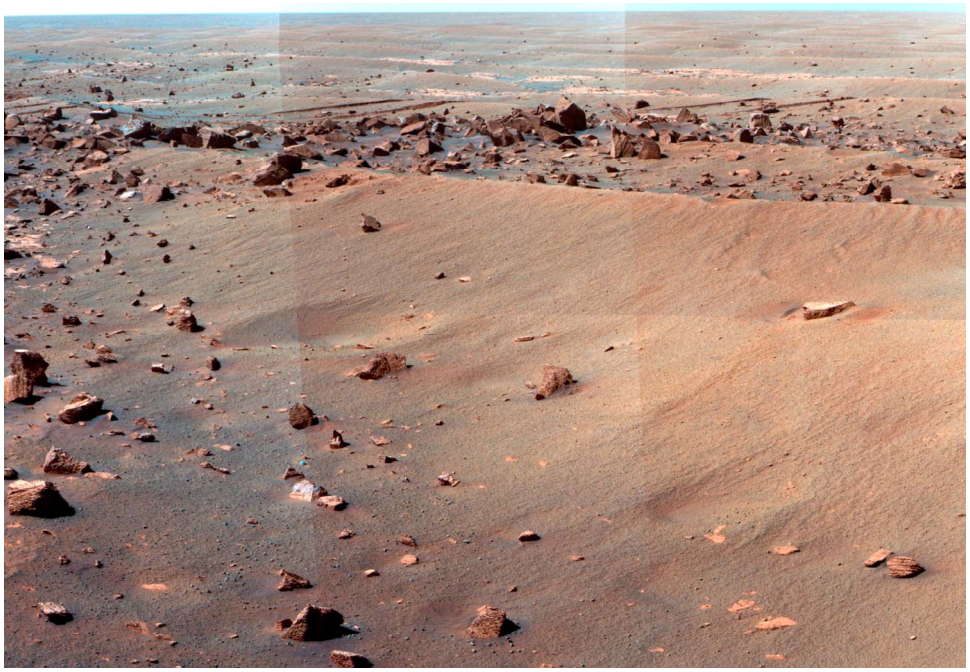

Figure 22. Pancam color mosaic of ripple, ejecta blocks and southeast ray acquired on sol 2170 looking toward the northeast when the rover was about 15 m south of the Concepción crater rim. Note ejecta blocks from the crater are superposed on the ripple. Circular depressions in the ripple were likely formed by ejecta impacting the ripple. Note secondary ripples that have modified the main ripple and the rover tracks in the background. Circular depression in the foreground is about 40 cm across.

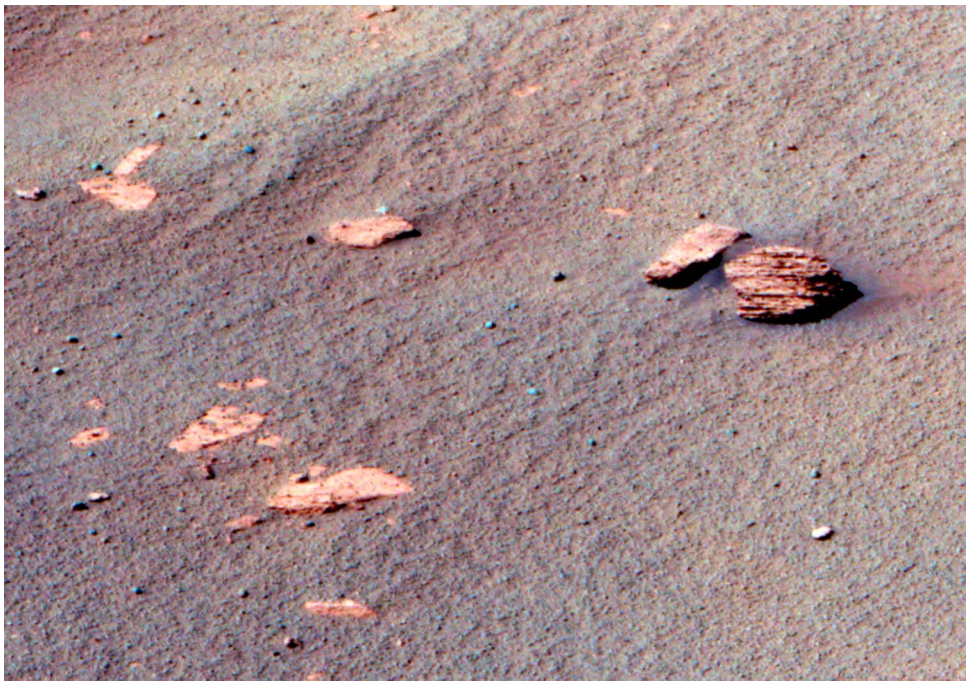

Figure 23. Close-up of near field of Pancam color mosaic shown in Figure 22 showing detail of soil surface. Note the absence of blueberries perched on the soil. Blueberries appear partially buried in soil which has a ridged appearance, suggesting that it is cemented. The lack of perched blueberries and the cemented surface suggests that they have been dispersed by the impact, consistent with the lack of hematite signature around large rayed craters in Meridiani Planum (Figure 25).

Figure 24. Pancam color image of sulfate block near the rim of Concepción crater showing large number of blueberries weathering out of the rock. In general, few blueberries are found perched on the ground around the crater (e.g., see surfaces away from the boulder), but this block appears to have shed blueberries surrounding it. Because the block was placed on the surface by the impact, the blueberries surrounding it provide a measure of how much eolian erosion has occurred since the impact (see section 6.4). The block is about 30 cm in diameter about 2.4 m south of the rover. The image was acquired on sols 2139–2142 when Opportunity was about 5 m north of Concepción crater.

higher thermal inertias and are composed of coarser-grained and/or blockier ejecta (compared with fine-grained ejecta and background sand and granules) [*McEwen et al.*, 2005; *Tornabene et al.*, 2006]. The bright nighttime thermal rays and ejecta are asymmetric, extending further to the east (Figure 25), suggesting that this was a low-angle impact from the west [e.g., *Gault and Wedekind*, 1978].

[23] HiRISE images of Ada (Figure 26) show it is a very fresh crater with minimal eolian modification (some eolian bed forms on its floor). The interior is unusual, exhibiting two bedrock layers, giving the crater a nested appearance as observed in some small (generally several km or less in diameter) lunar craters believed to have formed in a target with a weak layer over a strong layer [*Quaide and Oberbeck*, 1968]. The upper light-toned layer (order tens of meters thick) is likely the weak, sulfate Burns formation characterized by Opportunity [*Grotzinger et al.*, 2005]. The lower layer forms cliffs and sheds boulders, exposing a strong layer a couple of hundred meters beneath the Burns formation that has not yet been seen by Opportunity. Exposure of this deeper layer is broader to the east, similar to the ejecta asymmetry and also suggestive of an oblique impact from the west. Secondary craters and ejecta with fresh herringbone patterns can be traced 8 km north and south in the HiRISE images of the crater and much farther in nearby HiRISE images to the east and south. About 6 km south-southwest of, and 32 km south of Ada, secondary craters can be seen that are clearly superposed on the ripples (Figures 27 and 28). To the south, secondary craters from Ada cover the ripple crests and troughs in between (Figure 27). Further to the south, secondary craters in HiRISE color (Figure 28) show light-toned ejecta (presumably Burns Formation) superposed on top of the ripples and troughs. Ripples have not modified the Ada secondary craters. As a result, the superposition of secondary craters produced by Ada on the ripples indicates that Ada is younger than the latest phase of ripple migration at Meridiani Planum.

4.2. Unnamed 0.84 km Diameter Crater

[24] An unnamed 0.84 km diameter crater is the second of two larger, fresh-rayed craters in Meridiani Planum that have impacted into surfaces similar to those traversed by the Opportunity rover. This unnamed 0.84 km diameter crater is located about 40 km west of Victoria crater (Figure 25). Components of the ejecta and radiating rays from this crater also appear bright in nighttime THEMIS images indicating they have higher thermal inertias, and are interpreted to consist of coarser-grained and/or blockier ejecta (compared with other fine-grained ejecta, ray material, and background sand and granules) [*McEwen et al.*, 2005; *Tornabene et al.*, 2006]. A HiRISE image (Figure 29) of this unnamed crater shows it is fresh with some eolian modification (star dunes on its floor). The rim is composed of cliffs of light-toned layered material on the order of tens of meters thick that are likely the sulfate-rich Burns formation characterized by Opportunity [*Grotzinger et al.*, 2005]. Secondary craters and ejecta with fresh herringbone patterns can be traced for 10 km north and south of the main crater in the HiRISE image that includes the crater. About 9 km south of the crater, secondary craters are found in terrain with ripples similar to that which Opportunity has traversed (Figure 30). Secondary craters appear modified by ripples in this area, with distorted noncircular shapes, dark sand-filled interiors, and no obvious ejecta. Many secondary crater rims are discontinuous and ripples have overtaken them. In many cases, ripples extend beyond the crater to the north and south, but merge with and overtop the crater rims in between. These relations indicate that the secondaries are older than the ripples and that the 0.84 km diameter unnamed crater is older than the latest phase of ripple migration at Meridiani Planum.

5. Age of Ripple Migration

[25] Three largely independent methods are used to date the age of the latest phase of ripple migration at Meridiani Planum by (1) measuring only the freshest unmodified craters in a portion of a HiRISE image around Resolution crater, (2) estimating the age of Ada and the unnamed 0.84 km diameter crater from younger craters superposed on their continuous ejecta blankets, and (3) estimating the expected recurrence intervals of similar diameter fresh-rayed craters in the equatorial region of Mars compared with the two Meridiani craters.

[26] With the advent of the very high-resolution HiRISE images, crater counts and isochrons established from 1 km and larger craters, have been extended down to about 10 m diameter craters [*Hartmann and Neukum*, 2001; *Ivanov*, 2001; *Hartmann*, 2005]. In addition, small crater populations on very young impact crater ejecta are also about the

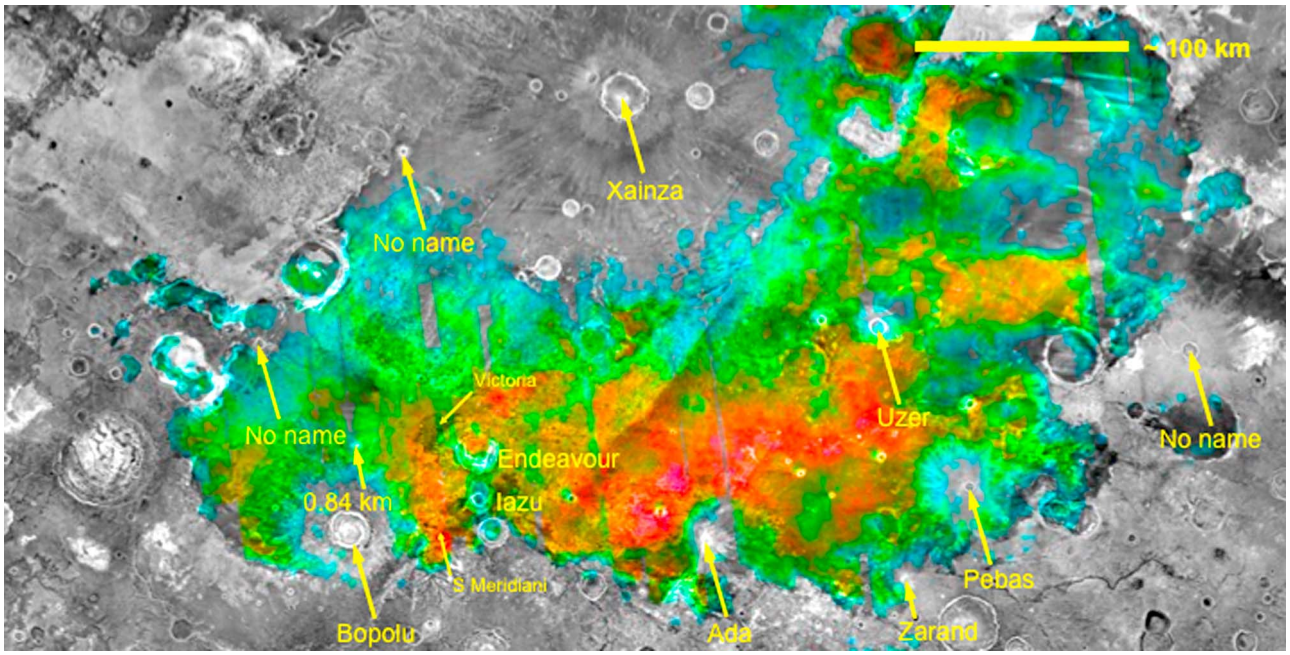

Figure 25. THEMIS nighttime image mosaic of Meridiani Planum showing the freshest and best preserved craters with TES-derived hematite concentration overlain in color. The location of Victoria crater is shown (the Resolution cluster is 2.3 km to the southwest) as are the two fresh-rayed craters, Ada (150 km to the east-southeast) and the 0.84 km diameter unnamed crater (40 km to the west), that have impacted into rippled surfaces similar to those traversed by Opportunity. Note how the hematite concentration is removed or reduced in and around (within the rays) of the fresh craters. Because the hematite concentration measured by TES is produced by the blueberry concretions left at the surface as a granule lag, the removal of the blueberries by mixing in ejecta and ray material or perhaps impact air blast would be expected for craters younger than the most recent phase of ripple migration. Note the asymmetric rays around Ada that have no hematite signature, consistent with this crater being younger than the latest phase of ripple migration. Note the 0.84 km diameter unnamed crater has a reduced hematite concentration, consistent with this crater forming before the latest phase of ripple migration so that some blueberries have been reexposed as a lag at the surface by saltation. THEMIS nighttime thermal images are at about 100 m/pixel; TES hematite concentration varies from >2% in blue to about 15–20% in red in ~3 × 6 km pixels from *Christensen et al.* [2001b].

same for craters down to about 10 m diameter used for establishing the isochrons [*Kreslavsky*, 2009] and observed impacts over the past several years have size-frequency distributions that match the isochrons to this size range [*Daubar et al.*, 2010]. As a result, deriving model ages from crater counts of small craters appears justified. In addition, small craters can be counted on the continuous ejecta of very fresh, larger craters to estimate the age of the impact event by comparison with isochrons that have been developed [*Hartmann*, 2005]. Craters superposed on young craters are also unlikely to be affected by secondaries from other younger craters.

[27] We note that over short time scales, the cratering rate varies by a factor of 4 due to the eccentricity of the orbit [*Ivanov*, 2001], which will add considerable uncertainty to ascribing an absolute age from the isochrons. In brief, for the last ~0.5×10^9 years Mars' orbit is elongated with an eccentricity e >0.05 (current eccentricity e = 0.09, varies from 0.0 to 0.14 in an oscillating manner with a gross period of ~2.2 Myr [*Armstrong et al.*, 2004; *Laskar et al.*, 2004]). The larger eccentricity brings Mars closer to the asteroid belt in aphelion where more asteroids have a chance to strike it. Hence, Hartmann's (2005) impact rate averaged for the time since lunar mare formation (~3.4 Ga) may be lower than the current (and recent, <0.5 Myr) impact rate. This has the effect of making ages, estimated with Hartmann's (2005) "average" isochrons, artificially older (less time needed to accumulate the same number of craters with higher-than-average impact rate), possibly by a factor of 2 [*Ivanov*, 2001].

[28] Use of small craters for chronology is problematic in other ways. First, they are easily erased by eolian or other surface processes, so the crater retention age is always a lower limit on the true age of the surface unit, but we are considering only very well-preserved craters here. Another problem is that the diameters of small craters are quite sensitive to target properties, resulting in potential errors of about a factor of 5 for craters smaller than ~30 m diameter [*Dundas et al.*, 2010], but we have no reason to believe that the target materials in the present study are unusual. The cumulative error in age estimates from all sources is likely between 1 and 2 orders of magnitude. Nevertheless, the relative age differences that are more important from this analysis should not be affected.

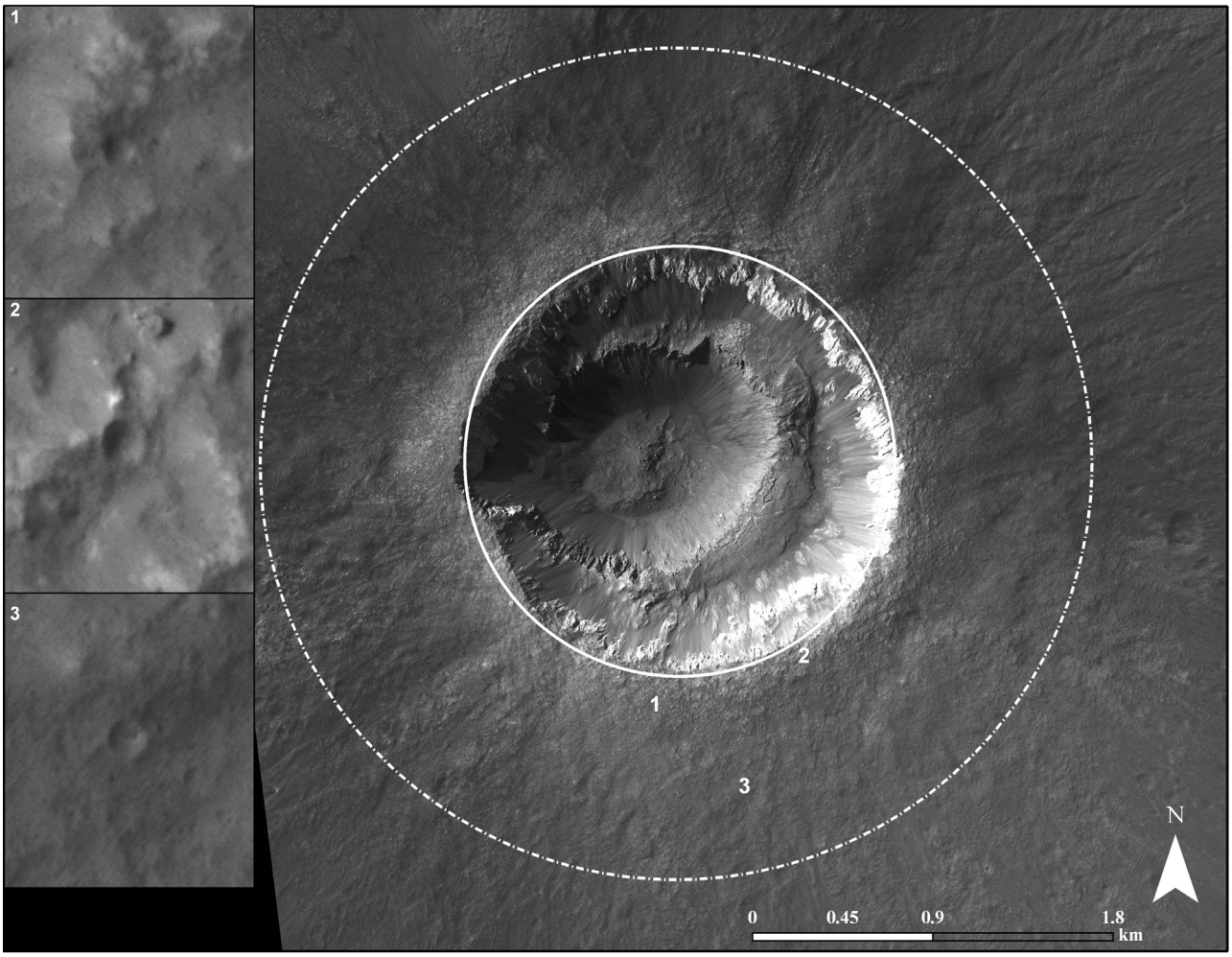

Figure 26. HiRISE image PSP_001348_1770 of the crater Ada, a 2.2 km diameter fresh-rayed crater about 150 km east-southeast of Victoria crater. Note unusual two-layer interior, with the bright, likely sulfate outcrop upper layer (tens of meters thick) and a strong lower layer. Asymmetry is consistent with an oblique impact from the west (also indicated by the asymmetry of the rays and ejecta seen in Figure 25). Also shown are three small craters (inset boxes are 32 m wide) on the continuous ejecta blanket (between the circles) that are fresh and bowl shaped (diameters in Table 2) and thus interpreted to be younger than the crater and distinct from many degraded craters that could have formed during emplacement of the ejecta. The size-frequency distribution of these small craters indicates the crater impacted ~50 ka.

[29] These methods are directed at the latest phase of ripple migration only, because the provenance of the basaltic sand that forms the ripples is unknown and its initial deposition at Meridiani Planum is poorly constrained. Measurement of all craters <250 m diameter on Meridiani indicates a fairly young surface (Late Amazonian) or crater retention age that is of order 10 Ma [*Lane et al.*, 2003] based on Hartmann's isochrons [*Hartmann*, 2005]. Because these craters formed in basaltic sand (and outcrop) that make up the surface and are in various stages of degradation [*Golombek et al.*, 2006a], the present surface, including the sand must have been transported to Meridiani (as no obvious protolith has been identified) before then. Because the sulfates of the Burns formation are Late Noachian to Early Hesperian [*Arvidson et al.*, 2006; *Hynek and Phillips*, 2008] and the Hesperian cratering record has been eroded away [*Lane et al.*, 2003; *Golombek et al.*, 2006a], it is possible that the sand forming the present surface of Meridiani Planum accumulated sometime during the Hesperian or Amazonian (after 3.6 Ga), but before about 10 Ma.

5.1. Small Unmodified Crater Age

[30] Although measuring the size-frequency distribution of all craters <250 m diameter suggests an age of ~10 Ma for the sand-modified surface at Meridiani, observations by Opportunity show that many of these craters have been modified to varying extents by the ripples and eolian activity [*Grant et al.*, 2006; *Golombek et al.*, 2006a]. To estimate when the ripples were last active, only craters that are clearly superposed on the ripples were counted. Craters interpreted to be younger than the ripples have continuous, unbroken circular rims that truncate ripple crests, show no signs of eolian modification or bed forms inside or on the rims, and have ejecta blocks that are superposed on the

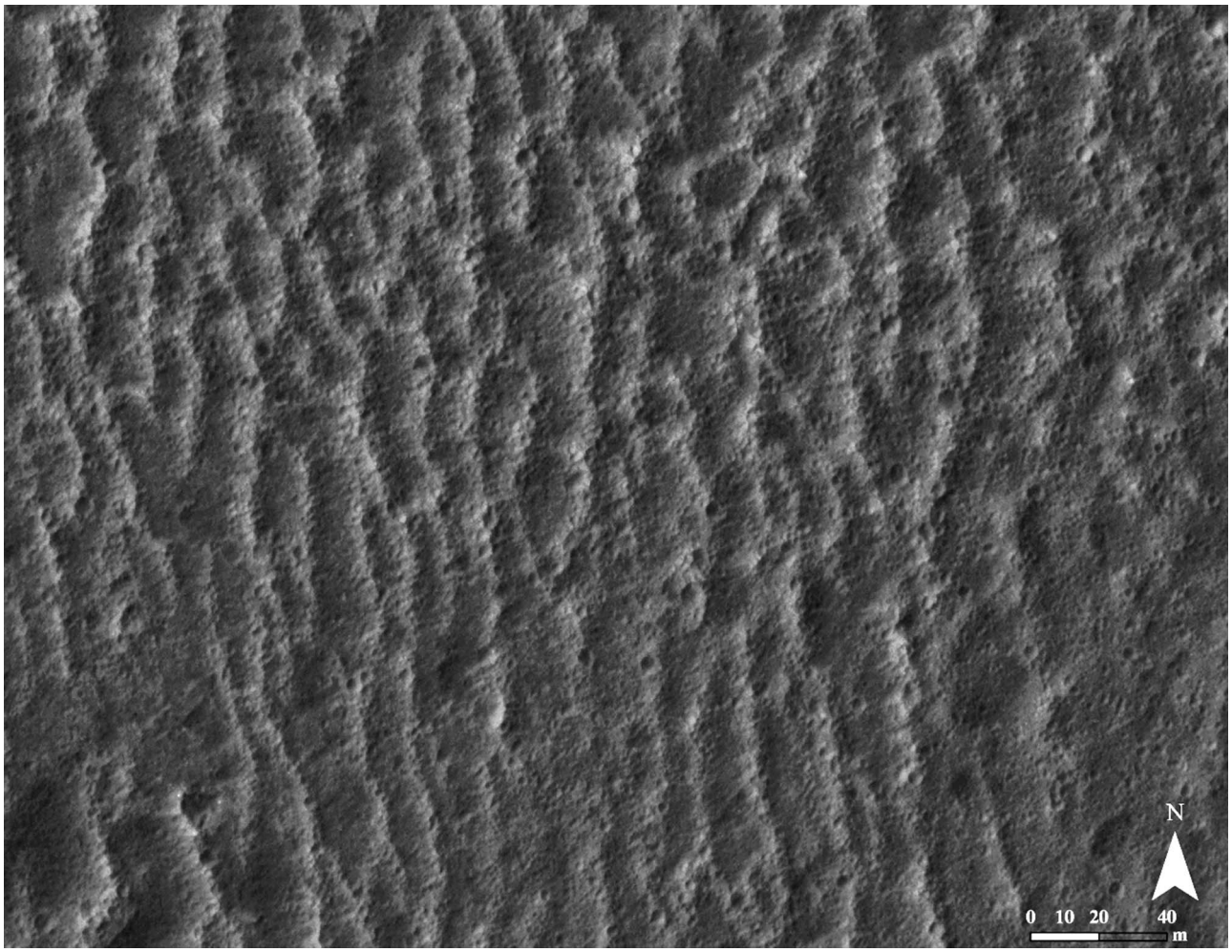

Figure 27. HiRISE image PSP_001348_1770 of secondary craters from Ada on ripples about 6 km south of the primary. Meter-sized secondaries are clearly superposed on and thus younger than the ripples, indicating that Ada impacted after the latest phase of ripple migration at Meridiani Planum.

ripples. An example of a fresh cluster with these characteristics is shown in Figure 31 (the Resolution cluster is obviously another example, Figure 1). Eight such craters were identified and their diameters measured (Table 2) in a 22.67 km^2 area of the southern portion of HiRISE image PSP_001414_1780, which includes part of Opportunity's traverse and the Resolution crater cluster (Figure 32). Two of these craters are clusters, for which we calculated an effective diameter (assuming it had not fragmented) using $D_{eff} = (\Sigma D_i^3)^{1/3}$ [*Ivanov et al.*, 2008]. The size-frequency distribution of craters (the cumulative number of craters normalized by area) define a model age of ~50 ka for the two largest diameter bins, which include the largest craters and clusters, with counting statistics that vary from ~20–80 ka for D > 7.81 m [*Hartmann*, 2005] (Figure 33). The cumulative size frequency distribution for craters smaller than 3.91 m diameter fall on the 10 ka isochron with uncertainties of 3–20 ka, suggesting a slightly older age for the largest craters or that smaller craters have been modified, eroded and/or missed. In any case, the uncertainties in the counting statistics of the two overlap considerably. Because the two largest bins include the largest craters and crater clusters and because the crater retention age represents the minimum age of the surface, we will assume the age of 50 ka represents when the ripples were last active (as they are clearly superposed on the ripples).

5.2. Larger, Fresh-Rayed Crater Age

[31] Fresh impacts on the continuous ejecta of Ada and the unnamed 0.84 km diameter rayed crater in Meridiani were counted to estimate their age. Because Ada is younger, and the unnamed 0.84 km diameter crater is older than the latest phase of ripple migration, their ages should bracket the age of the latest phase of eolian activity responsible for the north trending granule ripples. We assumed the continuous ejecta blankets extend to about 1 crater radius away from the rim [e.g., *Melosh*, 1989].

5.2.1. Ada Crater Age

[32] The entire continuous ejecta blanket of Ada was surveyed in the HiRISE image. Care was taken to distinguish degraded craters that could have formed during emplacement of the ejecta from subsequent, fresh craters with uplifted rims and bowl shapes that formed later. Three bowl-shaped craters with diameters of 4.3, 4.5 and 6 m (Table 2), and uplifted rims that appear superposed on the ejecta of Ada, were found on the continuous ejecta (Figure 26). The binned size fre-

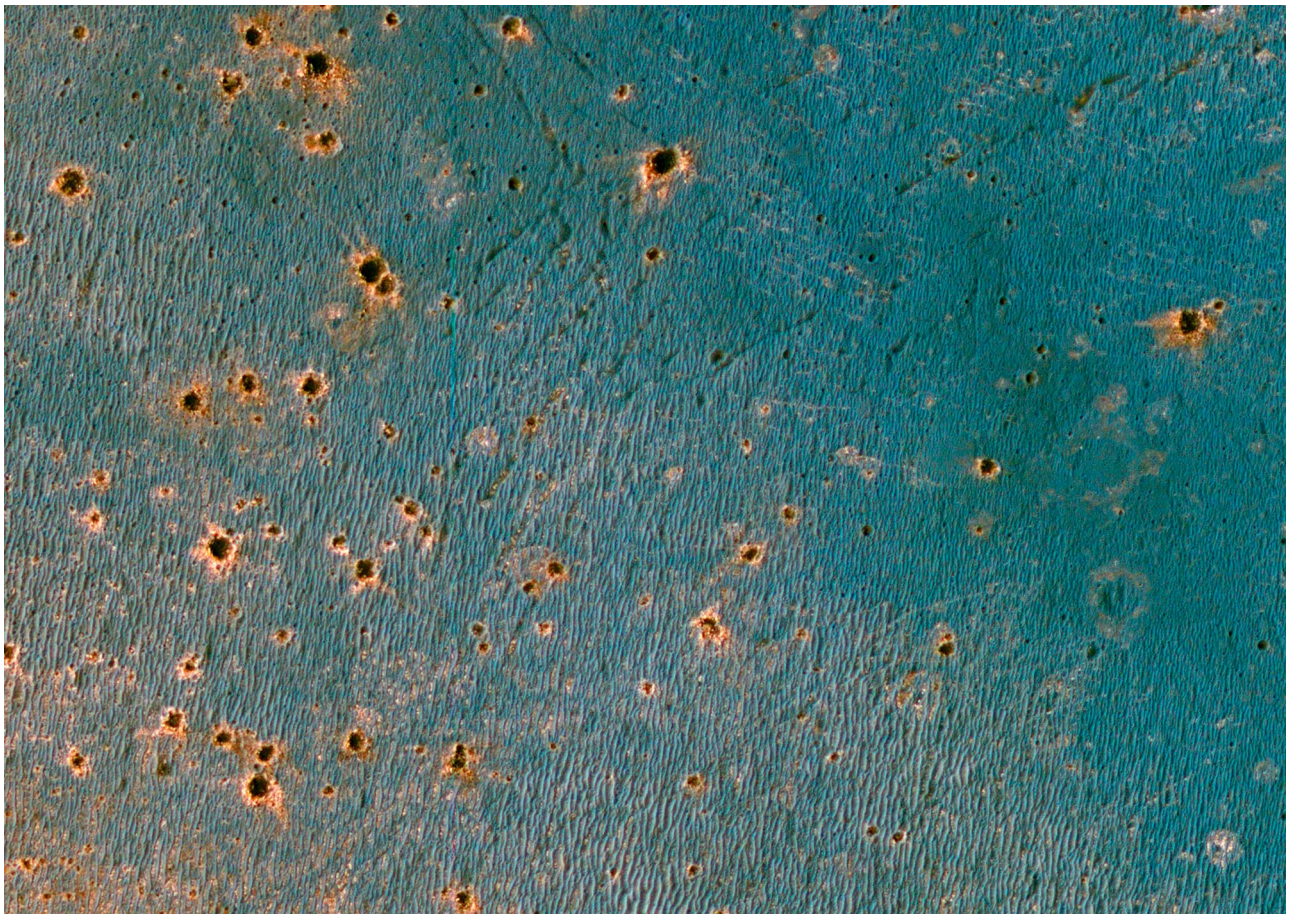

Figure 28. HiRISE image ESP_014178_1765 of secondary craters from Ada on ripples about 32 km south of the primary. Largest craters are about 8 m in diameter and have bright rims consistent with their impacting into light-toned sulfate bedrock. Craters are clearly superposed on the ripples, indicating Ada is younger than the latest phase of ripple migration at Meridiani Planum.

quency distribution of these craters falls on the ~50 ka isochron of *Hartmann* [2005], with counting statistics that vary from ~20–80 ka for diameters >3.91 m (Figure 33), arguing that Ada formed about 50 ka (assuming that no superposed small craters have been erased). Because secondaries from Ada are superposed on the ripples at Meridiani, the latest phase of ripple migration occurred prior to ~50 ka. Even given the large uncertainties in estimating ages using crater counts of a very small number of small-diameter craters (note statistical uncertainties in Figure 33), the derivation of the same model age from both the measurement of all unmodified craters in the HiRISE image that includes the Resolution cluster (section 5.1), as well as craters impacted on the ejecta blanket of Ada, argues that this result is moderately robust. Further, because both of these different areas yield a similar age estimate, ripple migration appears roughly coeval at both areas (separated by ~150 km), suggesting that to first order ripple migration occurred at the same time through much of Meridiani Planum.

5.2.2. Unnamed 0.84 km Diameter Crater Age

[33] Five bowl-shaped craters (Table 2) with uplifted rims that appear superposed on the ejecta of the unnamed 0.84 km diameter crater were found on its continuous ejecta blanket (Figure 29). The binned size frequency distribution of craters with D > 3.91 m fall on the ~200 ka isochron of *Hartmann* [2005], with error bars spanning 100–800 ka (Figure 33). The cumulative number of craters per km^2 for other diameter bins fall between 200 ka and 100 ka. Because crater retention ages represent the minimum age of the underlying terrain (continuous ejecta blanket), this indicates that the unnamed 0.84 km diameter crater impacted at ~200 ka. Because secondaries from the unnamed 0.84 km diameter crater are modified and degraded by the ripples at Meridiani, the latest phase of ripple migration occurred after ~200 ka. Coupled with the age derived from Ada and the unmodified craters in the HiRISE image that includes Resolution crater, this result suggests that the latest phase of ripple migration occurred between model ages of ~200 ka and ~50 ka across over 200 km of Meridiani Planum.

5.3. Recurrence Rates of Fresh-Rayed Craters

5.3.1. Introduction

[34] Although rayed craters are common on the Moon, rayed craters were first identified on Mars via their distinctive bright and dark rays in THEMIS thermal images [*McEwen et al.*, 2005]. The thermal contrast in the rays may generally extend for up to ~200 crater radii (up to 2000 km for the largest, 14 km diameter Corinto crater) and includes

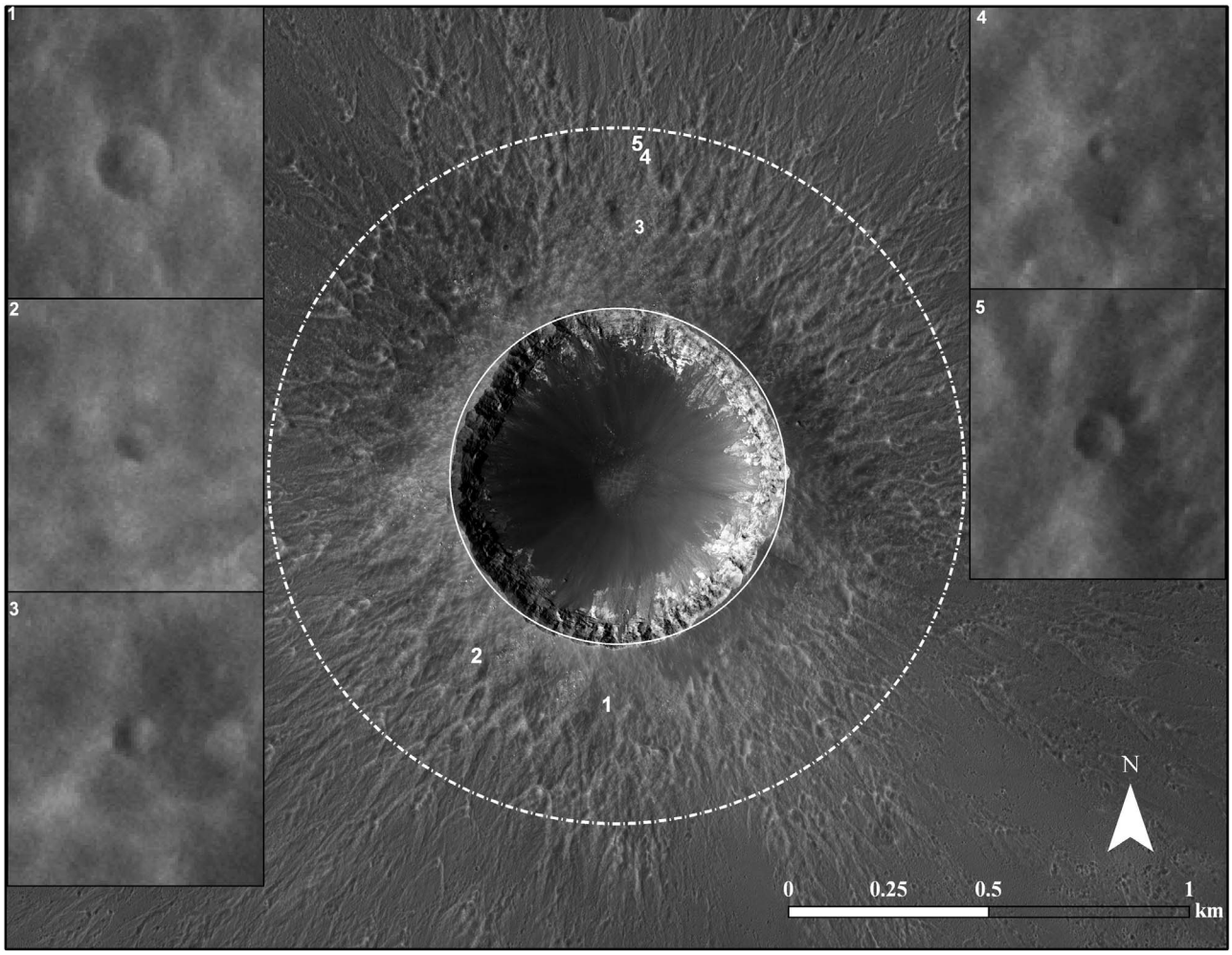

Figure 29. HiRISE image PSP_005990_1780 of unnamed 0.84 km diameter fresh-rayed crater about 40 km west of Victoria crater. Note light-toned, likely Burns formation outcropping at the inner rim and fresh rays and star dunes on the crater floor. Also shown are five small craters (inset boxes are 23 m wide) on the continuous ejecta blanket (between the circles) that are fresh and bowl shaped (diameters in Table 2) and thus interpreted to be younger than the crater and distinct from many degraded craters that could have formed during emplacement of the ejecta. The size-frequency distribution of these small craters indicates the crater impacted ~200 ka.

both low and high thermal inertia facies and extensive populations of secondary craters [*Tornabene et al.*, 2006]. Crater rays are geomorphically young features (easily erased by eolian processes) and so rayed craters are among the youngest craters, with rays degrading with time. They appear to have formed preferentially in moderate thermal inertia and albedo terrain and are best recognized on surfaces with consistent intermediate temperatures. This suggests that the thermophysical properties of the target material are important in the formation of thermally distinct rays [*Tornabene et al.*, 2006]. Since their discovery in THEMIS images, there has been a concerted effort to identify and image all fresh-rayed craters ≥ 1–2 km in diameter with HiRISE. Because the presence of thermally distinct rays indicates a youthful or well-preserved crater, the production function for craters [*Hartmann and Neukum*, 2001; *Ivanov*, 2001] can be used with other constraints to calculate the recurrence interval expected for craters of a particular size range over some area on Mars [e.g., *McEwen et al.*, 2005]. In this section, all fresh-rayed craters ≥ 1–2 km diameter are classified according to their thermophysical properties and eolian modification to estimate the recurrence interval of Ada and the unnamed 0.84 km diameter Meridiani crater as a way of checking the ages derived from the crater counts described in sections 5.1 and 5.2.

5.3.2. Fresh-Rayed Craters in the Midlatitude of Mars

[35] In the effort by the HiRISE team to image all fresh-rayed craters larger than 0.5 km diameter, HiRISE images have been acquired of 52 fresh craters that have been identified in the THEMIS thermal images with distinctive ejecta patterns and diameters of 0.5–4 km. Of these, 32 craters are within 30° of the equator, which is conveniently about half of the surface area of Mars and eliminates potential complicating factors at high latitudes such as ground ice and cryoturbation [e.g., *Kreslavsky*, 2009]. Each of these craters was located, surveyed, and diameter measured in the HiRISE images. In addition, the eolian modification of each crater was

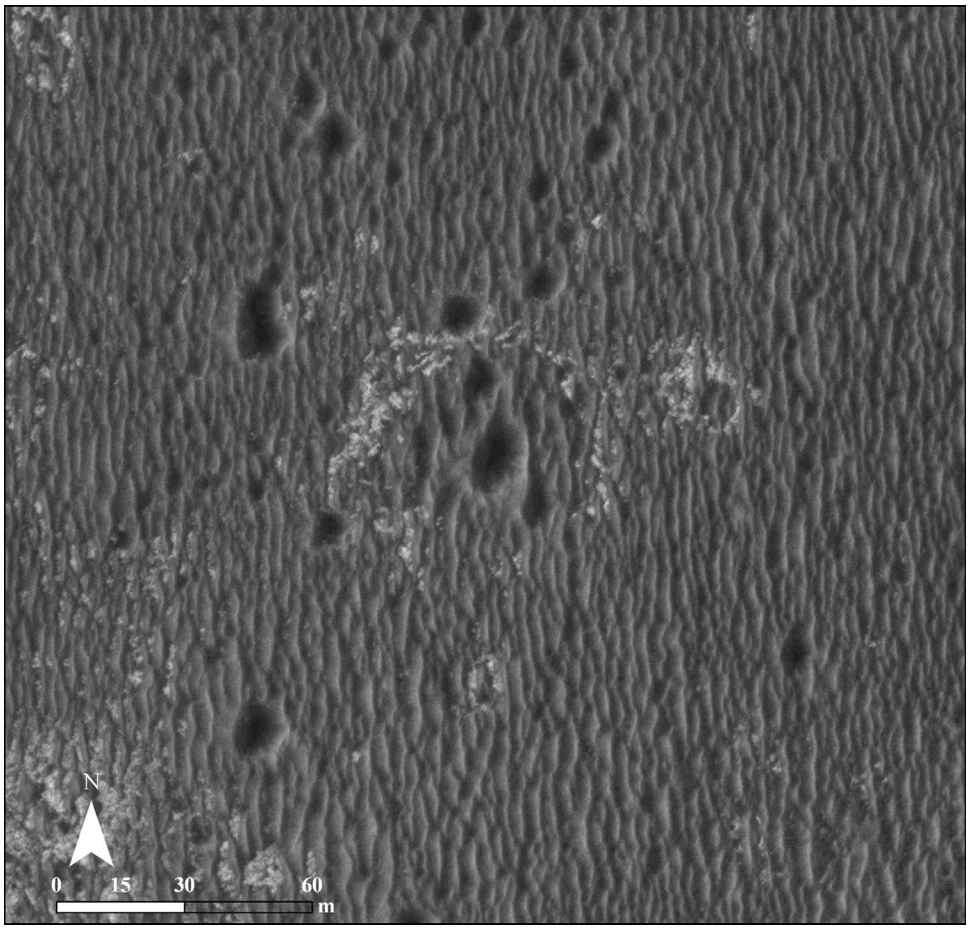

Figure 30. HiRISE image PSP_005990_1780 of secondary craters (largest crater about 11 m in diameter) from unnamed 0.84 km diameter fresh-rayed crater about 9 km south of the primary. Note distorted non-circular crater shapes, dark sand-filled interiors, and discontinuous rims that merge with ripples, some of which extend farther to the north and south. These relations indicate that the ripples migrated and modified the craters after they impacted, and thus the 0.84 km unnamed crater is older than the latest phase of ripple migration at Meridiani Planum.

evaluated and their thermophysical properties cataloged (Table 3).

5.3.2.1. Eolian Modification

[36] For each of the 32 craters in the catalog, the degree of eolian modification was ascribed to a relative qualitative scale of 1 to 5, with 1 being least modified and 5 being most modified (Table 3). In addition to evaluating the eolian deposits within each crater, the freshness of the rays (if any), secondary craters and ejecta were also evaluated with more degraded examples assumed to be older. Because there are no definitive examples of eolian bed forms within craters that have formed in the past 10 years (see section 6.4.1), the simplest assumption is that the older the crater, the greater the accumulation of eolian bed forms relative to its size, and thus craters with a greater fraction of their floor covered by eolian bed forms should, to first order, be older. This assumes that eolian activity and the accumulation of eolian material is the same everywhere on Mars, which is almost certainly not the case, but it is hoped that within broad bounds that the degree of eolian deposition and modification of the craters can be used as a general proxy for age.

[37] Craters without any identifiable eolian deposits within or around them were placed in class 1 (least modified). Craters with relatively few eolian bed forms of limited size were classed as 2 (Ada is an example of this classification, see Figure 26). Craters of this class also have fresh secondaries and ejecta rays without eolian deposits or modification. Craters with greater accumulation of eolian deposits, including those with moderate size star dunes on their floors were classed as 3 (the unnamed 0.84 km diameter rayed crater is an example of this class, see Figure 29). Craters of this class have secondaries that have been modified by eolian bed forms or have bed forms on adjacent ejecta. Craters with substantial dunes deposited in their interiors that cover a large portion of their floors are classed as 4. Craters of this class commonly have secondary craters that have eolian deposits within them and bed forms on adjacent ejecta. Class 5 craters have extensive eolian bed forms that cover most of their interiors, more degraded rays, and secondaries that have been heavily modified or filled by eolian deposits.

[38] Results of classifying the 32 fresh craters 0.5 to 4 km diameter within ±30° using this scale displayed in histogram

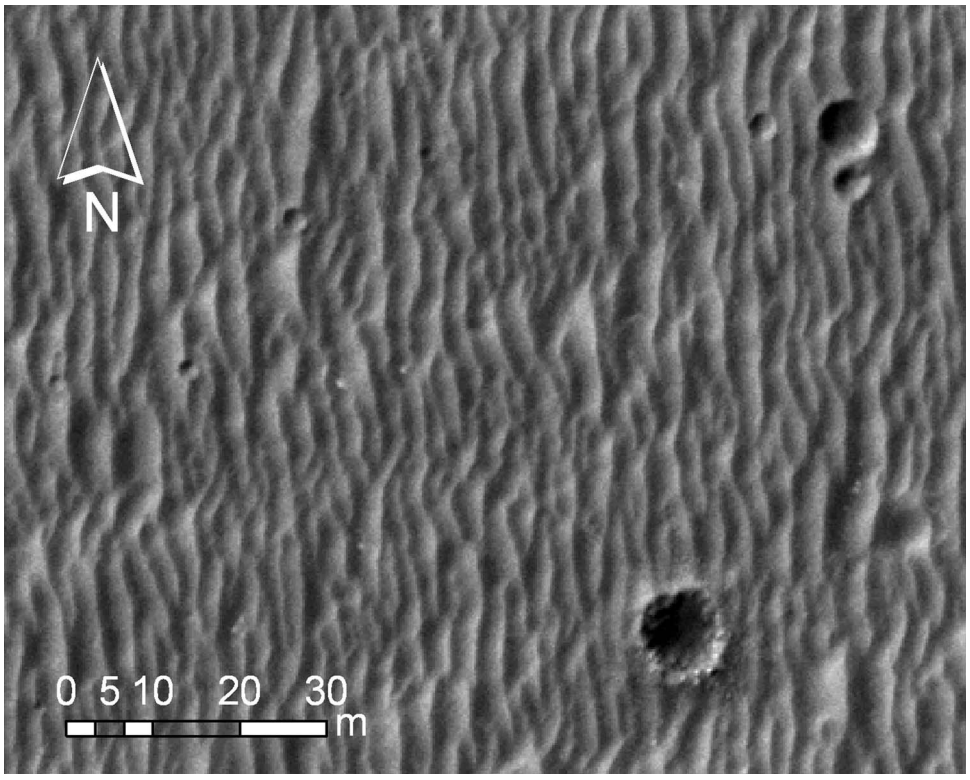

Figure 31. HiRISE image PSP_009141_1780 of fresh crater cluster about 8 km east-southeast of the Resolution crater cluster on Meridiani Planum. The largest crater is about 10 m in diameter with a blocky rim and ejecta blocks on the surface. These craters clearly truncate the north trending ripples and show no signs of being modified significantly by eolian activity. These attributes indicate that these craters are younger than the latest phase of ripple migration at Meridiani and similar in age to the Resolution crater cluster.

form are shown in Figure 34. Eleven craters fall in class 3 of the sample, with eight in class 2 and seven in class 4. Only one crater is in class 1 (the least modified) and five are in class 5 (the most modified). There appears to be a size bias with the largest craters being the most modified and the smallest craters (0.5 km diameter) being the least modified, which may be partially a resolution effect, due to the difficulty of identifying eolian deposits in small craters (see also section 6.4.1). In this classification scheme, Ada is the least modified and youngest 2.2–4 km rayed crater and the unnamed 0.84 km diameter Meridiani crater is the 5th to 13th least modified (youngest) 0.8–4 km diameter rayed crater in the equatorial region of Mars. However, the catalog may not include all small diameter craters (<1–2 km diameter) because of their size, so this could modify the results. Because of these uncertainties, they are considered representative only and will only be used in example calculations in section 5.3.3.

5.3.2.2. Thermophysical Properties

[39] Because the larger thermal rayed craters on Mars are more readily detected and appear to form preferentially in moderate thermal inertia and albedo terrain on Mars [*Tornabene et al.*, 2006], all thirty two 0.5–4 km diameter fresh-rayed craters within ±30° of the equator were classified by their thermophysical properties. Most of the surface area of Mars (~80%) falls into 3 main thermal inertia and albedo units [*Mellon et al.*, 2000; *Putzig et al.*, 2005]. Most larger rayed craters are found in moderate to high thermal inertia and intermediate to high-albedo unit C that is dominated by duricrust with various abundances of rocks and bright dust. Moderate to high thermal inertia and low-albedo surface unit B is relatively dust free and composed of dark eolian sand and/or increased abundance of rocks. The third main thermal inertia and albedo unit (unit A) of Mars has high albedo and very low thermal inertia (unit A) and is dominated by potentially thick bright red dust with low rock abundance. Of the 32 craters in the catalog, 17 are in unit C, 11 in unit B, and 4 are at the margins of unit A. Thermal Emission Spectrometer (TES) thermal inertia where small rayed craters are found varies from 50 to 320 J/m^2 K s$^{0.5}$ in the work of *Mellon et al.* [2000] and 70–330 J/m^2 K s$^{0.5}$ in higher-resolution *Putzig et al.* [2005] data. TES albedo [*Christensen et al.*, 2001a] varies from 0.10 to 0.28. About 60% of the terrain on Mars within ±30° of the equator has thermal inertia and albedo within these values; because the equatorial area considered constitutes about half of the surface area of the planet, our sample represents 30% of the surface of Mars.

5.3.3. Recurrence Intervals

[40] To calculate the recurrence interval for craters of a certain diameter, the *Hartmann and Neukum* [2001] production function as reported by *Ivanov* [2001] in cumulative number of craters per km^2 was multiplied by 30% of the area of Mars (about 6×10^7 km^2). Because the production

Table 2. Crater Diameters in Size-Frequency Distributions

Crater ID	Diameter (m)
Fresh Craters on PSP_001414_1780[a]	
1	D_{eff} = 9.4[b]
2	1.5
3	2.3
4	2.05
5	2.25
6	9.8[c]
	5.58
	1.3
	1.55
	1.2
	2.45
	2.9
	1.55
	3.2
	7.05
	3.95
	D_{eff} = 11.785
7	2.82
8	2.18
Craters on Ada Ejecta[d]	
1	4.5
2	5.95
3	4.3
Craters on Unnamed 850 m Diameter Crater Ejecta[e]	
1	7.05
2	3.45
3	3.95
4	2.6
5	4.6

[a]Measured over 22.67 km^2 area.
[b]Resolution crater cluster in Table 1.
[c]Crater cluster partially shown in Figure 31.
[d]Measured over 9.9 km^2 area.
[e]Measured over 1.81 km^2 area.

function of *Ivanov* [2001] is reported for the past 3.4 Ga, the cumulative number of craters is divided by 3.4 Ga and then inverted to get the average time between crater impacts (recurrence interval). To get the recurrence interval for craters within a certain size range, the crater number reported by *Ivanov* [2001] of the largest diameter crater in the range is first subtracted from the crater number of the smallest diameter crater in the range. Results indicate that 2.2–4 km diameter and 0.8–4 km diameter craters should form roughly every 400 ka and 30 ka, respectively, on this portion of Mars.

[41] Because Ada is the least modified and thus a likely candidate for the youngest 2.2–4 km diameter crater within the sampled portion of Mars, the calculated recurrence interval suggests that Ada impacted in the past 400 ka, which is consistent with the ~50 ka age for Ada derived from the size-frequency distribution of fresh craters on its continuous ejecta (section 5.2.1). Because Ada secondaries are superposed on Meridiani ripples, this result is also consistent with the latest phase of ripple migration occurring prior to ~50 ka. Because the unnamed 0.84 km diameter Meridiani rayed crater represents the 5th to 13th youngest (least modified) 0.84–4 km diameter rayed crater in the sampled portion of Mars, it is estimated to have impacted sometime between 120 ka and 400 ka years ago. However, the HiRISE inventory is likely incomplete for craters of this size (below about 1 km diameter) and state of preservation, so the impact event was likely older. This result is consistent with the ~200 ka model age derived from the size-frequency distribution of fresh craters on its continuous ejecta blanket. Because secondary craters from the unnamed 0.84 km diameter Meridiani crater are modified and overprinted by ripples, this result is also consistent with the latest phase of ripple migration at Meridiani occurring after ~200 ka.

6. Discussion

6.1. Ripple Migration From Three Methods

[42] Three largely independent methods have been used to constrain the latest phase of granule ripple migration at Meridiani Planum. The size-frequency distribution of only unmodified impact craters observed in a HiRISE image that includes the Resolution crater cluster suggests that craters younger than the plains ripples formed in the past ~50 ka and thus ripple migration occurred prior to ~50 ka. The 2.2 km diameter fresh-rayed crater, Ada, has secondary craters superposed on the ripples and so impacted after the latest phase of ripple migration. The size-frequency distribution of fresh craters on its continuous ejecta blanket indicate an impact age of about 50 ka, which is also consistent with stagnation of ripple migration since this time. The unnamed 0.84 km diameter fresh-rayed crater has secondary craters that have been modified by ripples and so impacted prior to the latest phase of ripple migration. The size-frequency distribution of fresh craters superposed on its continuous ejecta blanket indicate that it impacted about 200 ka and that the latest phase of ripple migration was after this time. Finally the recurrence intervals for fresh craters 0.5–4 km diameter in the equatorial region of Mars with similar thermophysical properties and varying degradation are consistent with Ada forming in the past 400 ka and the unnamed 0.84 km crater forming between 120 ka and 400 ka. All three methods indicate that the latest phase of ripple migration at Meridiani Planum occurred between ~200 ka and ~50 ka.

6.2. Evidence for Relatively Old Granule Ripples

[43] Granule ripples such as those at Meridiani Planum have surfaces covered with grains that are too coarse to saltate, but that can be driven in creep by a flux of finer, saltating sand that also characterizes the bulk of ripple interiors [e.g., *Sharp*, 1963]. A prerequisite for granule ripple migration, then, is an abundant supply of loose, saltating sand to drive the coarse grains in creep, in order to move the granule ripple crests slowly downwind. Without an abundant supply of saltating fine grains, granule ripples will not move, even during strong wind events. Investigations into granule ripples on Mars by the MER rovers show that surfaces of coarse sand and granules (overlying interiors of very fine sand) are cohesive and indurated, and this contributes to their resistance to reactivation by the wind [*Sullivan et al.*, 2005, 2007, 2008]. At Meridiani, several lines of evidence suggest that the large north trending granule ripples are relatively old features, old enough and large enough to have guided finer saltating sand along intervening troughs, leading to smaller secondary ripples or cuspate cross ripples in these locations. Most recent eolian activity has involved only shifting accumulations of a rather

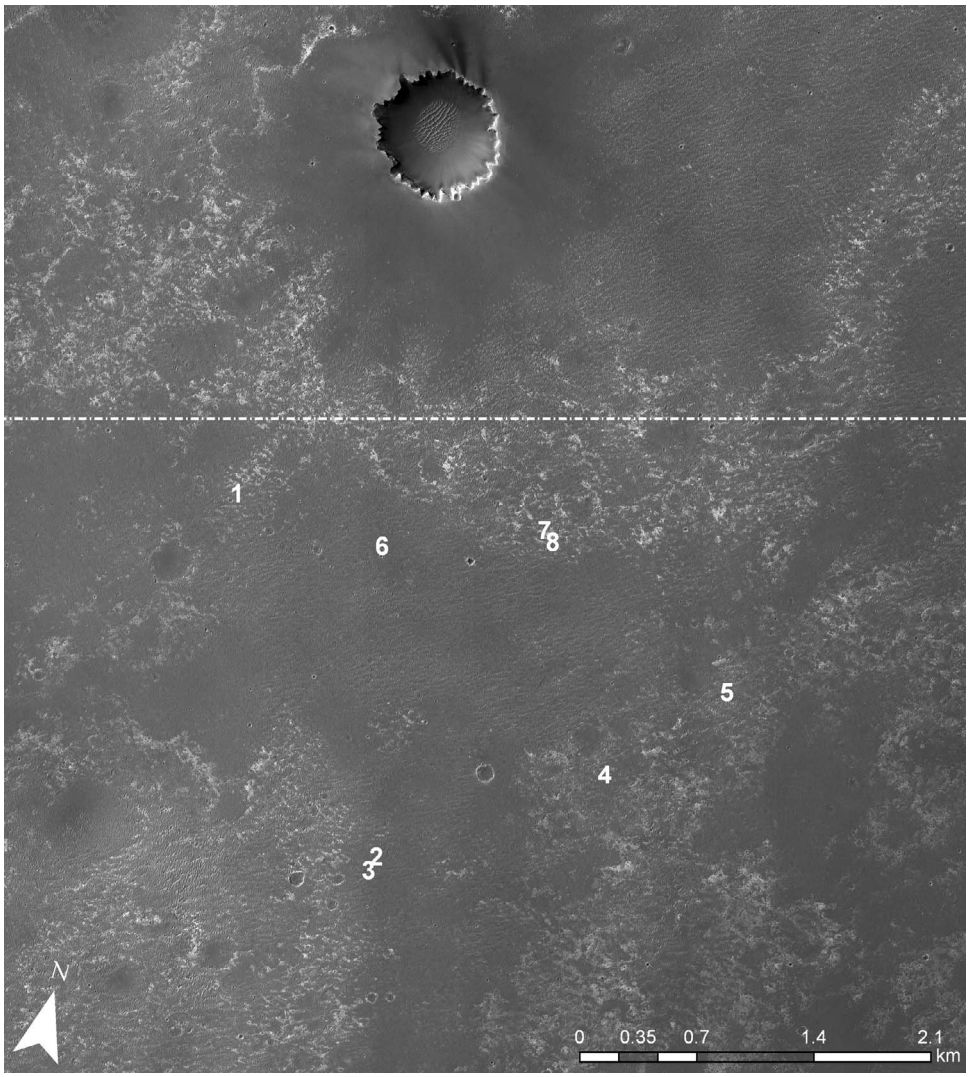

Figure 32. Southern portion of HiRISE image PSP_001414_1780 showing unmodified craters interpreted to be younger than the latest phase of ripple migration at Meridiani Planum. Numbers refer to craters and crater clusters whose diameters are reported in Table 2. Crater 1 is the Resolution crater cluster, about 2.3 km southwest of Victoria crater (the large crater with smooth, dark annulus to the north), and the cluster shown in Figure 31 is crater 6.

sparsely distributed population of very fine sand (forming short-wavelength, ordinary ripples in isolated accumulations) and the erosion of bedrock by this activity [*Sullivan et al.*, 2007]. The stagnation of the larger north trending granule ripples, combined with their durable surface of relatively resistant hematite spherules, has resulted in Burns formation ejecta blocks being planed off to conform to the rippled surface, establishing that the granule ripples have been more stable than blocks of sulfate outcrop [*Sullivan et al.*, 2007]. Finally, the east flanks of many large north trending ripples appear layered (e.g., see cross sections in Rayleigh crater in Figure 6), suggesting older layers from previous episodes of ripple migration from the east [*Sullivan et al.*, 2007]. These observations all suggest that the large north trending ripples at Meridiani are relatively old features formed in an older wind regime [*Sullivan et al.*, 2005] and are consistent with an age greater than ~50 ka.

[44] Extremely slow migration of granule ripples on Mars has also been inferred from observations of granule ripple migration on Earth [*Zimbelman et al.*, 2009]. Granule ripple migration was measured at Great Sand Dunes National Park after a particularly strong wind storm in September 2006. The observed saltation-induced creep rate was extrapolated to Mars by considering the frequency of high winds observed at the Viking landers and accounting for differences in atmospheric density, gravity, and wind friction speed between Earth and Mars [*Zimbelman et al.*, 2009]. Results suggest that it should take hundreds to thousands of years for a 25 cm high ripple to migrate 1 cm. In this extrapolation, migrating Meridiani ripples of order 1 m to overprint secondary crater rims would require on the order of tens to hundreds of thousands of years, which is also consistent with our estimates of the latest phase of ripple migration at Meridiani occurring before ~50 ka.

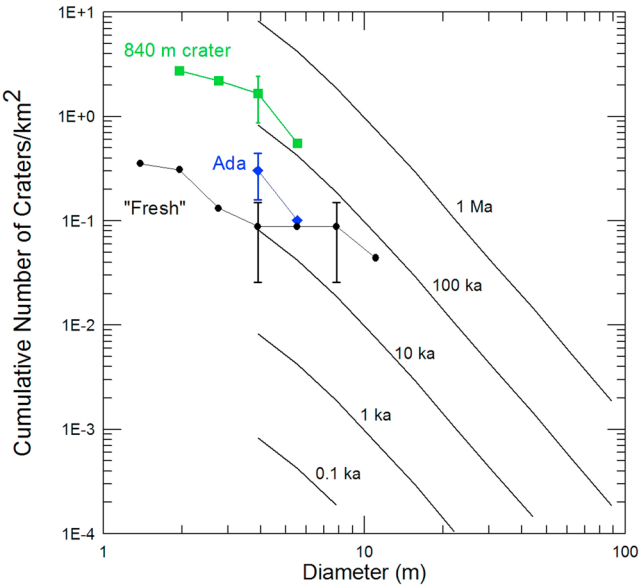

Figure 33. Cumulative size-frequency distributions of different crater populations at Meridiani Planum described in the text. The log-log plot is the diameter (D) versus the cumulative number of craters (N) with ± $[N(>D)]^{1/2}$ uncertainty of 1σ at N(D) > 3.9 m and the isochrons of *Hartmann* [2005]. The three size-frequency distributions shown are (1) unmodified craters in a 22.67 km^2 area of Meridinai Planum (Figure 32) marked "fresh" in black circles that includes the Resolution crater cluster, (2) craters superposed on the continuous ejecta blanket of Ada crater (9.9 km^2) marked "Ada" in blue diamonds (Figure 26), and (3) craters superposed on the continuous ejecta blanket of the unnamed 0.84 km diameter crater (1.81 km^2) marked "840 m" in green squares (Figure 29). Distributions 1, for the two largest diameter bins, and 2 fall on the 50 ka isochron indicating ripple migration occurred before then, and distribution 3 is about 200 ka, indicating ripple migration occurred after then. The uncertainty in isochron age from the counting statistics varies from about 20 ka to 80 ka for distributions 1 for D of 7.81 m and 2 for D of 3.91 m and from 80 ka to 300 ka for distribution 3 for D of 3.91 m. The lack of small single craters in distribution 1 with diameters between 3.91 m and 7.81 m may be due to the older (20 to 80 ka) age of accumulation of the 2 largest impacts with D_{eff} > 7.81 m (both of them are clusters) or because smaller craters are more easily modified, eroded, and/or missed. Crater diameters are in Table 2.

6.3. Hematite Concentration and Rayed Craters at Meridiani

[45] The main science factor that led to the selection of Meridiani Planum as a MER landing site is the presence of strong TES spectral signatures indicating up to 15–20% of the surface covered by the mineral hematite (coarse grained), which typically forms in the presence of liquid water [*Christensen et al.*, 2001b; *Golombek et al.*, 2003] (Figure 25). After landing, the hematite signature was found to result from the concentration of hematite concretions (blueberries) that have been weathered out of the sulfate Burns formation and accumulated as a lag on the surface [*Christensen et al.*, 2004; *Soderblom et al.*, 2004]. Given that fresh-rayed craters are very young and the rays result from high-velocity ejecta impacting the surface [*Tornabene et al.*, 2006], it would be expected that such recent impacts should show evidence of having affected the concentration of blueberries at the surface and thus there should be changes in the hematite concentration near such craters.

[46] If Ada crater is younger than the latest phase of ripple migration at Meridiani, as indicated by its secondaries, the impact of the crater and its ejecta would be expected to dramatically disperse or bury blueberries. Granules sitting on top of the surface prior to the impact would be mixed in the ejecta and debris flows and associated air blasts (atmosphere compressed by the shock wave [e.g., *Melosh*, 1989]) might be able to disperse them. As a result, no blueberries would be expected around the crater or its rays, and thus there should be little to no hematite detected by TES. In contrast, if the unnamed 0.84 km diameter rayed crater impacted before the latest phase of ripple migration, subsequent ripple migration should have partially restored the blueberries as a granule lag, so the TES hematite concentration should be lower than adjacent areas unaffected by the impact, but should still be detected. This is exactly what is shown in Figure 25, which overlays the TES hematite concentration on the THEMIS nighttime thermal image mosaic of the Meridiani region. Hematite concentration is below the TES detection limit (<~2% [*Christensen et al.*, 2001b]) or absent around Ada with the same asymmetric pattern as the rays and ejecta, which preferentially extend to the east (from a low-angle impact from the west). Hematite concentration around the unnamed 0.84 km diameter crater is lower than adjacent areas, but still detected. These observations further support the relative ages derived for the unnamed 0.84 km diameter and Ada craters with the latest phase of ripple migration occurring in between their impacts. Other fresh impact craters at Meridiani Planum appear to have similarly decreased hematite concentration around them (including Concepción, see section 3) indicating that the processes that have dispersed or buried the blueberries are common during impact cratering on Mars.

6.4. Time Scale for Small Craters on Meridiani Planum and Mars

[47] Observations of small craters at Meridiani and fresh-rayed craters elsewhere on Mars enable the development of a time scale for their formation based on their morphology, eolian modification, and preservation of rays. To develop such a time scale, first the very youngest craters that have impacted Mars in the past 10 years are discussed. Next a very fresh crater cluster with both light and dark ejecta rays in southern Meridiani is described, and compared to Concepción crater, which has some dark ejecta rays. Finally, relatively fresh craters that appear older than ripple migration are discussed.

6.4.1. Craters Formed in the Past 10 Years

[48] To provide a constraint on the rate of eolian modification of craters, 58 HiRISE images, each containing one or more impact craters verified to have formed since May 1999 were examined. The timing and location of these recent craters came from independent analyses of Mars Orbiter Camera wide angle [*Malin et al.*, 2006] and MRO CTX images showing dark spots that are believed to have

Table 3. Fresh-Rayed 0.5–5 km Diameter Craters on Mars

Latitude, Longitude (deg)	Diameter (km)	Relative Age[a]	Thermal Inertia - Albedo Unit		Thermal Inertia of *Mellon et al.* [2000] (J/m^2 K $s^{0.5}$)	Thermal Inertia of *Putzig et al.* [2005] (J/m^2 K $s^{0.5}$)	Albedo[b]	HiRISE Image
			Mellon et al. [2000]	*Putzig et al.* [2005]				
−24.74, 257.78	0.5	1	C	C	127	224	0.23	PSP_004886_1550
14.05, 128.74	0.5	2	C	C	190	232	0.235	PSP_006842_1940
−2.15, 165.75	0.5	2	A	A	54	115	0.272	PSP_008291_1780
−22.35, 220.03	0.5	2	C	C	123	157	0.257	PSP_008500_1575
20.32, 177.31	0.5	3	A	A	73	73	0.266	PSP_009121_2005
14.55, 114.09	0.6	2	C	C	207	242	0.231	PSP_005735_1945
−18.32, 182.78	0.7	3	C	C	133	167	0.234	PSP_008475_1615
−2.25, 353.79	0.84	3	B	B	179	233	0.139	PSP_005990_1780[c]
−24.88, 49.41	0.85	4	B	B	249	309	0.12	PSP_009983_1550
−11.55, 103.79	1	3	B	B	180	236	0.183	ESP_012605_1685
4.77, 46.19	1	3	A	A	77	90	0.269	PSP_002230_1850
−16.77, 348.84	1	4	B	B	206	298	0.136	PSP_008548_1630
29.96, 49.44	1.05	3	C	C	135	165	0.246	PSP_008506_2105
−3.74, 59.16	1.15	2	B	B	173	213	0.144	ESP_012356_1760
−10.44, 24.56	1.15	4	D	B	102	172	0.126	PSP_005145_1690
−14.16, 38.63	1.2	3	B	B	261	227	0.14	PSP_002204_1655
−7.90, 142.05	1.6	3	C	C	172	269	0.239	PSP_010863_1720
−21.44, 260.62	1.4	3	C	C	180	264	0.246	PSP_008459_1585
15.54, 159.21	1.5	4	C	C	313	319	0.224	PSP_003940_1955
−33.99, 238.68	1.7	2	C	C	167	235	0.223	PSP_005045_1455
−12.88, 113.20	1.75	2	B	B	160, 144	247, 200	0.1680.163	ESP_013976_1670
−13.41, 48.18	2	4	C	C	165	233	0.214	PSP_009205_1665
−20.87, 184.36	2	4	C	C	155	207	0.229	PSP_009622_1590
−3.05, 356.79	2.2	2	B	B	139	263	0.132	PSP_001348_1770[d]
22.48, 151.44	2.25	3	A	A	127	114	0.271	PSP_009834_2025
13.27, 157.21	2.5	5	C	C	208	092	0.236	PSP_006841_1935
14.51, 108.92	2.8	5	C	C	233	290	0.242	PSP_008438_1945
−25.84, 127.14	2.9	3	B	B	226	258	0.152	PSP_008543_1540
28.57, 318.76	3	4	B	B	192	301	0.14	PSP_006479_2090
4.71, 134.35	3	5	C	C	204	267	0.245	PSP_006710_1850
−28.67, 226.93	3	5	C	C	255	271	0.226	PSP_003608_1510
14.88, 123.29	4	5	C	C	207	299	0.236	PSP_001660_1950

[a]Relative age from youngest (1) to oldest (5) according to morphologic criteria in text.
[b]Albedo from TES [*Christensen et al.*, 2001a].
[c]Unnamed 0.85 km diameter crater in Meridiani.
[d]Ada.

formed from dust mobilization and removal associated with the impacts. Craters colocated with the spots were imaged in subsequent MOC Narrow Angle, THEMIS, and CTX, and HiRISE images, and shown to have attributes of pristine impacts, such as crisp rims and dark floors and, where present, dark ejecta and blast zones. Because of the youth of these craters, an a priori assumption had been that bed forms would not be present within them, consistent with the low frequency of winds above threshold in the thin Martian atmosphere. This was largely borne out in our analysis. Out of the 58 images, 33 had craters too small, too shadowed, or too dark to discern any interior details. Of the remaining 26, 14 showed no clear indication of bed forms. The remaining 12 images showed craters with mottled clumps of material on their floors, some organized circumferentially interior of the crater walls. This material may therefore be deposits of unorganized impact debris and slump deposits. There is no compelling evidence for bed forms at the resolution of HiRISE. A relatively recent crater not in this set, from PSP_007899_2015, shows obvious ripples. However, there is some question as to whether this crater formed in the last decade, as the earliest MOC WA angle image of the area (M07-02993), taken in 1999, had a generally low albedo, making the identification of dark spots difficult. Therefore, bed forms are rare or completely absent within craters with ages of a decade or less.

6.4.2. Craters Formed in the Past Decades: Fresh Cluster in South Meridiani

[49] A fresh crater cluster in southern Meridiani Planum, about 50 km south of Victoria crater, was imaged in color by HiRISE (Figure 35). This cluster impacted into terrain that is similar to what Opportunity has traversed with north trending ripples and exposures of light-toned outcrop (presumably Burns Formation) in the troughs. The cluster consists of about 20 craters with the largest crater about 16 m diameter. The craters in the cluster are oriented along a west-northwest azimuth with the largest crater located near the west-northwest end, suggesting that the impactor came from the east-southeast. Most of the larger craters have dark ejecta rays that extend up to several crater radii away. Opportunity's exploration of Concepción crater, which has dark ejecta rays (section 3), shows that they are produced by shadows from rays of blocky sulfate ejecta. The craters appear unmodified by eolian activity and are clearly superposed on the ripples.

[50] Most of the craters large enough to excavate beneath the ripples to the sulfates (including those with dark rays) have bright yellowish deposits as part of their ejecta. The

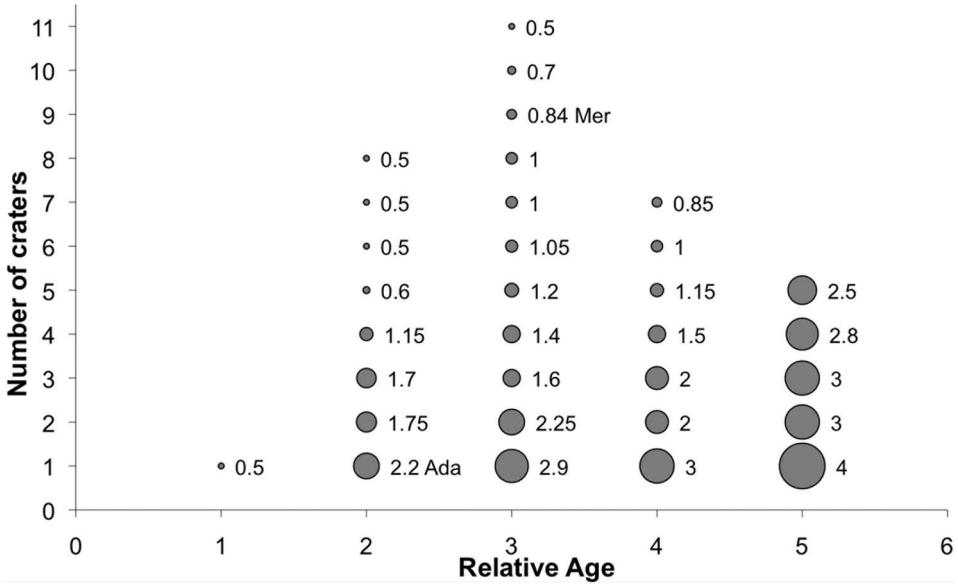

Figure 34. Histogram of the number of craters (diameter shown) within each relative age bin of the 32 fresh-rayed 0.5–5 km diameter craters within 30° of the equator of Mars. Relative age is from the least modified (1), assumed to be the youngest, to the most modified (5), assumed to be the oldest, based on crater morphology and the degree of eolian modification (see text for discussion). Plot shows that Ada is the youngest 2.2–4 km rayed crater and the unnamed 0.84 km diameter Meridiani crater (0.84 Mer) is the 5th to 13th least modified (youngest) 0.8–4 km diameter rayed crater in the equatorial region of Mars.

bright yellowish deposits are most likely extremely fine-grained or comminuted sulfate outcrop deposits. Because Opportunity has not seen any such deposits associated with craters, they likely have been removed fairly quickly by the wind. Evidence for removal of this bright material by the wind is found in the darker troughs in Figure 35, suggesting that modern winds funneled down the troughs (also note the west-northwest oriented lighter and darker bands indicating interaction with secondary ripples) preferentially removing the dust compared with the brighter west side of ripples. The extensive eolian abrasion of the Burns formation by saltating sand has likely produced copious quantities of sulfate dust that has been removed from Meridiani. The effective diameter [*Ivanov et al.*, 2008] for this cluster is 18.6 m, which for the 30% area that contains the fresh-rayed 0.5–5 km diameter craters in section 5.3, suggests a recurrence interval of about 6 days. Given the presence of the bright yellowish dust at this cluster and its absence elsewhere (including the older craters to be discussed), this cluster is probably several decades old.

6.4.3. Craters Formed in the Past Millennium: Concepción Crater

[51] Concepción appears to be the freshest (youngest) crater visited by either rover; it appears to truncate the ripples, has blocky ejecta, and has dark ejecta rays that extend several crater radii to the southeast and south, (Figure 18). Comparing the morphology, degree of eolian modification, and freshness of Concepción crater with the south Meridiani and Resolution crater clusters suggests that it is intermediate in age between them. Concepción appears fresher and less modified by eolian activity than the Resolution crater cluster, but lacks the bright yellowish pulverized sulfate deposits in its preserved ejecta. This suggests that Concepción is older than the south Meridiani cluster (estimated to be decades old) but younger than the Resolution crater cluster, which likely impacted tens of thousands of years ago (<100 ka, see section 6.4.4). From these loose limits, Concepción crater probably formed on the order of thousands of years ago.

6.4.4. Craters Formed Tens of Thousands of Years Ago

[52] The Resolution crater cluster is clearly younger than the north trending ripples, which were last active roughly 50–200 ka. The lack of any obvious rays around Resolution, the common modification of the craters by secondary ripples, and the slightly more degraded appearance compared with Concepción crater, all suggest that it is older than Concepción. Because Concepción crater is estimated to be thousands of years old with ripple migration occurring before fifty thousand years ago, the Resolution crater cluster is likely on the order of tens of thousands of years old, but <50 ka.

[53] Similar in age and perhaps slightly older is Ada and its secondaries, which has been estimated to be about 50 ka. For small secondaries impacting in sand, the craters appear as small shallow bowls (Figure 27). In other locations with larger craters that have excavated sulfate outcrop, the secondaries have bright rims and dark centers (Figure 28). The larger ones have blocky ejecta and what look like the remnants of light and sometimes dark ejecta rays. The dark interiors likely result from dark sand and the rays have probably been degraded with time from their initial state. The morphologic state of Ada secondaries appears consistent with their age of about 50 ka. Other unmodified craters that are younger than ripple migration measured in section 5.1 also share these morphologic attributes (e.g., Figure 31), which is consistent with their forming in the past 50 ka.

Figure 35. HiRISE color image PSP_009563_1770 of fresh crater cluster in southern Meridiani Planum. Largest crater is about 16 m in diameter, and its location at the west-northwestern edge of the cluster indicates that the impactor fell from the east-southeast (north is up). Larger craters show dark rays, likely shadowed and shaded blocky ejecta, and bright ejecta deposits, likely to be pulverized sulfate rock that is dispersed by the wind with time. The effective diameter [*Ivanov et al.*, 2008] for this cluster is 18.6 m, which for the area of Mars for which recurrence intervals have been calculated indicates a recurrence time of roughly 6 days. Given the presence of the bright yellowish dust at this cluster and its absence elsewhere and comparison to older craters discussed in the text, this cluster is probably several decades old. Location of crater cluster shown as S Meridiani in Figure 25.

6.4.5. Craters Formed Hundreds of Thousands of Years Ago

[54] The morphologies of craters that formed prior to the latest phase of ripple migration at Meridiani Planum are distinct from those that are younger. These older craters still may appear relatively fresh, but on closer inspection of the HiRISE image, their rims are modified by ripples, their shapes are less circular and more distorted, their interiors filled with various amounts of dark sand, and their ejecta is generally less distinct. Older eroded craters of this class are the secondaries of the unnamed rayed 0.84 km diameter crater west of Opportunity shown on Figure 30. Rims of these craters have been heavily modified by ripples and their interiors filled with dark sand. This crater has been estimated to have impacted ~200 ka and thus its secondaries have been largely modified by the latest phase of ripple migration at Meridiani Planum.

[55] A cluster of craters that have been partially modified by the north trending ripples at Meridiani Planum is the Kaikos crater cluster, first visited by Opportunity on sol 1950 (Figure 36). The Kaikos cluster is about 3.5 km southsouthwest of Victoria and 1.5 km from the Resolution cluster. The Kaikos cluster is composed of about 77 craters, 4 of which are larger than about 5 m diameter. The largest crater, Nereus is about 9 m in diameter and was visited by Opportunity on sol 2009. Kaikos and Nautilus craters (the latter imaged on sol 2011) are about 6 m in diameter. The cluster appears elongated in a northwest direction, with the largest crater toward the northwest, which suggests that the impactor fragmented as it fell from the southeast. The rims of these largest craters appear blocky in the HiRISE image, but there are no rays and no distinct ejecta away from the craters. On close inspection of the HiRISE image, several ripples appear to merge with the crater rims, suggesting that these craters are partially modified by the ripples.

[56] Images from Opportunity also suggest that these craters have been somewhat modified by ripples and eolian activity. Pancam color images show the craters have blocky rims with sandy interiors (Figure 37). Ripples appear to have merged with the crater rims (e.g., southeastern rim of Kaikos), but ejecta blocks appear to be partially planed off parallel to the surface (e.g., Nerius). Morphometric mea-

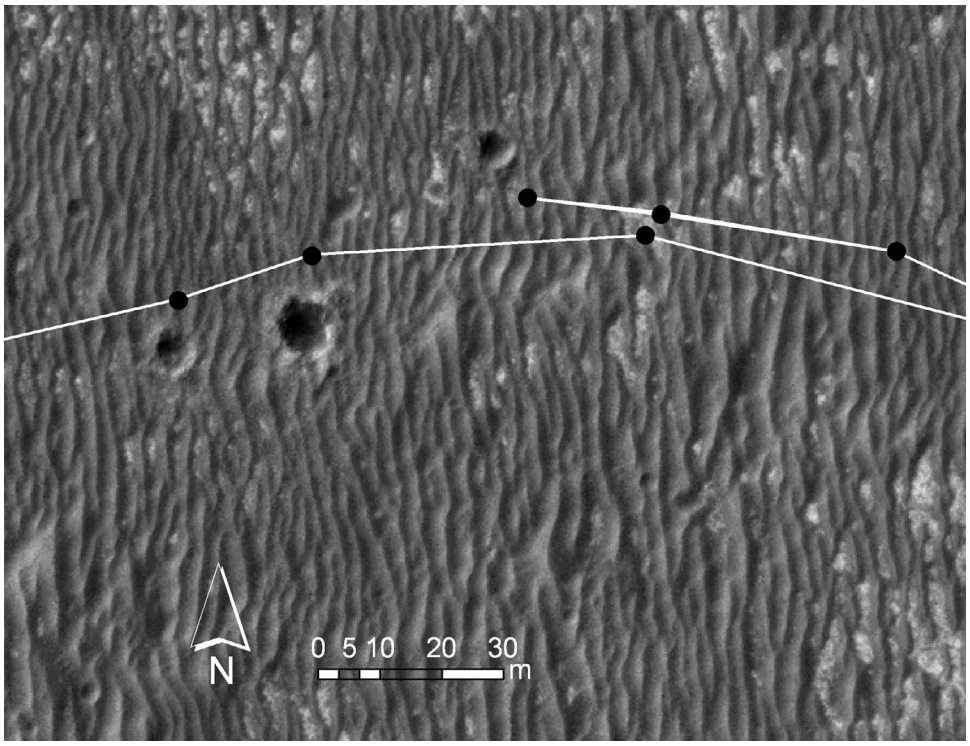

Figure 36. HiRISE image ESP_012820_1780 of the Kaikos crater cluster first visited by Opportunity on sol 1950 in southern Meridiani Planum. The Kaikos cluster is about 3.6 km south-southwest of Victoria and 1.4 km from the Resolution cluster. Kaikos crater (6 m in diameter) is the furthest east and was imaged on sol 1950. Nereus is the largest crater (9 m in diameter) and was imaged on sol 2009. Nautilus crater (6 m in diameter) is to the west and was imaged on sol 2011 (black dots are rover image locations). The rims of these craters appear somewhat blocky in this image, but on close inspection several ripples appear to merge with the crater rims, suggesting that these craters are partially modified by the ripples. Measurements of crater depth indicate that all three craters have depth/diameter ratios near 0.2, as would be expected for fresh hypervelocity impact craters. The partially ripple-modified nature of these craters suggests that they impacted during ripple migration around 100 ka. The diameter of 77 craters between 9.2 and 1 m were measured in the HiRISE image, yielding an effective diameter [*Ivanov et al.*, 2008] of 12.7 m. The distribution of the craters can be fit within an ellipse 285 m × 205 m oriented to the northwest. Because the largest craters are at the northwest end of the ellipse, the impactor likely fell from the southeast. The size-frequency distribution of craters in the cluster is similar to type 2 events in which a cascade of fragmentation events occurs for impactors with density 1.8–3 g/cm^3 [*Ivanov et al.*, 2008].

surements indicate all three craters have depth/diameter ratios near 0.2 as would be expected for fresh hypervelocity impact craters, indicating that the total thickness of sand in them is relatively thin (of order a few tens of centimeters). Dark pebbles are scattered across the surface of all three craters, suggesting that similar to other fresh craters, these dark pebbles are fragments of the impactor (which in this case would likely be exogenic). The partially ripple-modified nature of these craters suggests that they are younger than the unnamed 0.84 km diameter secondaries estimated to be 200 ka, but older than the unmodified secondaries of Ada estimated to be 50 ka, which suggests that the Kaikos cluster is roughly 100 ka.

[57] Two relatively fresh craters that have been modified by ripples in Meridiani Planum are located about 4 km west-northwest (cluster) of and 15 km south-southwest (doublet) of Victoria crater. Both craters have dark rays in HiRISE image ESP_016644_1780. The cluster is composed of >250 craters dispersed over several hundred meters, with the largest 3 craters 20–30 m in diameter (Figure 38). Most of the craters have dark interiors and the larger craters have eolian bed forms, suggesting that they are partially filled with dark sand. Ejecta blocks can be resolved around the larger craters, suggesting that like Concepción, the dark rays are produced by shadows and shading from blocky ejecta. Careful inspection of the crater rims shows that many have been overprinted by the north trending ripples, indicating that this cluster formed prior to the latest phase of ripple migration or >200 ka.

[58] The doublet crater is composed of two side by side craters about 30 and 40 m in diameter that form one depression with a septum between (Figure 39). The interior has eolian bed forms and smaller craters nearby are dark floored, suggesting that sand has been deposited in their interiors. Ejecta blocks are resolved around the crater and follow some of the rays. The rays around this crater are light toned. Inspection of the rays shows they appear to be composed of light-toned sulfate outcrop blocks that have

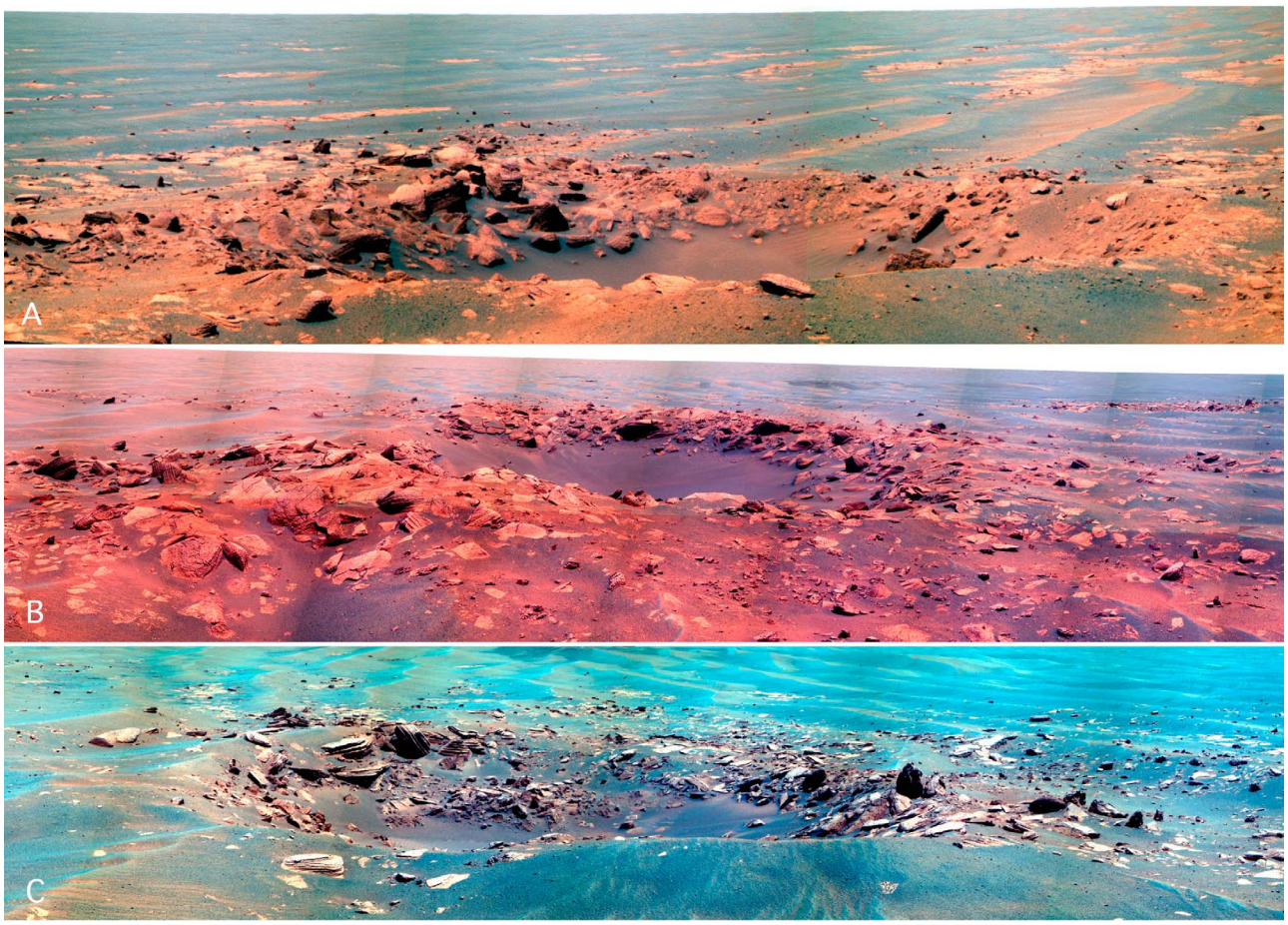

Figure 37. Pancam color image mosaics of (a) Kaikos, (b) Nereus, and (c) Nautilus craters, the three largest craters in the Kaikos cluster. The craters are relatively fresh, but the rims appear somewhat smooth, some ejecta blocks appear partially planed off parallel to the surface, and ripples merge with the crater rims, suggesting that the craters have been partially modified by the ripples.

been planed off with few shadows, suggesting that saltating sand has had enough time to wear the blocks down to the level of the surroundings. North trending ripples extend through the ejecta and heavily modify the rims of smaller companion craters. These relations suggest that this crater is older than the Kaikos cluster and thus of order many hundreds of thousands of years old. If true, this suggests that saltating sand has been abundant enough to physically erode ejecta since then.

6.5. Implications for Climate and Erosion

[59] Three independent methods indicate that the latest phase of ripple migration at Meridiani Planum occurred prior to ~50 ka, but after ~200 ka. So far, evidence of saltation and migration of dunes in the current era on Mars is very limited, despite dedicated searches for this activity in the spatially and temporally growing database of high-resolution orbital imagery, as well as in situ by the MER vehicles [*Zimbelman*, 2000; *Edgett and Malin*, 2000; *Malin and Edgett*, 2001; *Williams et al.*, 2003; *Williams*, 2006; *Fenton*, 2006; *Bourke et al.*, 2008; *Geissler et al.*, 2008, 2010; *Sullivan et al.*, 2008; *Silvestro et al.*, 2010; M. Chojnacki et al., Orbital observations of contemporary dune activity in Endeavor crater, Meridiani Planum, Mars, submitted to *Journal of Geophysical Research*, 2010]. This suggests that migration of the current dune population on Mars might have been more common prior to orbiter observations, in an era when conditions were more favorable to saltation of sand by the wind. The very limited evidence for bed form migration in the modern era suggests that periods of increased dune migration might exist as discrete episodes in recent geological history, interspersed with periods of very low activity. Induration of bed forms during periods of reduced activity would contribute additional resistance to reactivation at later times [*Sullivan et al.*, 2008]. These speculations of intermittent dune activity are also consistent with extraordinarily slow long-term erosion rates determined for the landing sites in the Amazonian [e.g., *Arvidson et al.*, 1979; *Golombek and Bridges*, 2000; *Golombek et al.*, 2006a].

[60] Observations of craters and estimates of their age further underscores what could be relatively rapid modification of the landscape over short periods when disturbed by an impact, even though ripple migration has been inactive for the past 50 ka and the cumulative modification of the

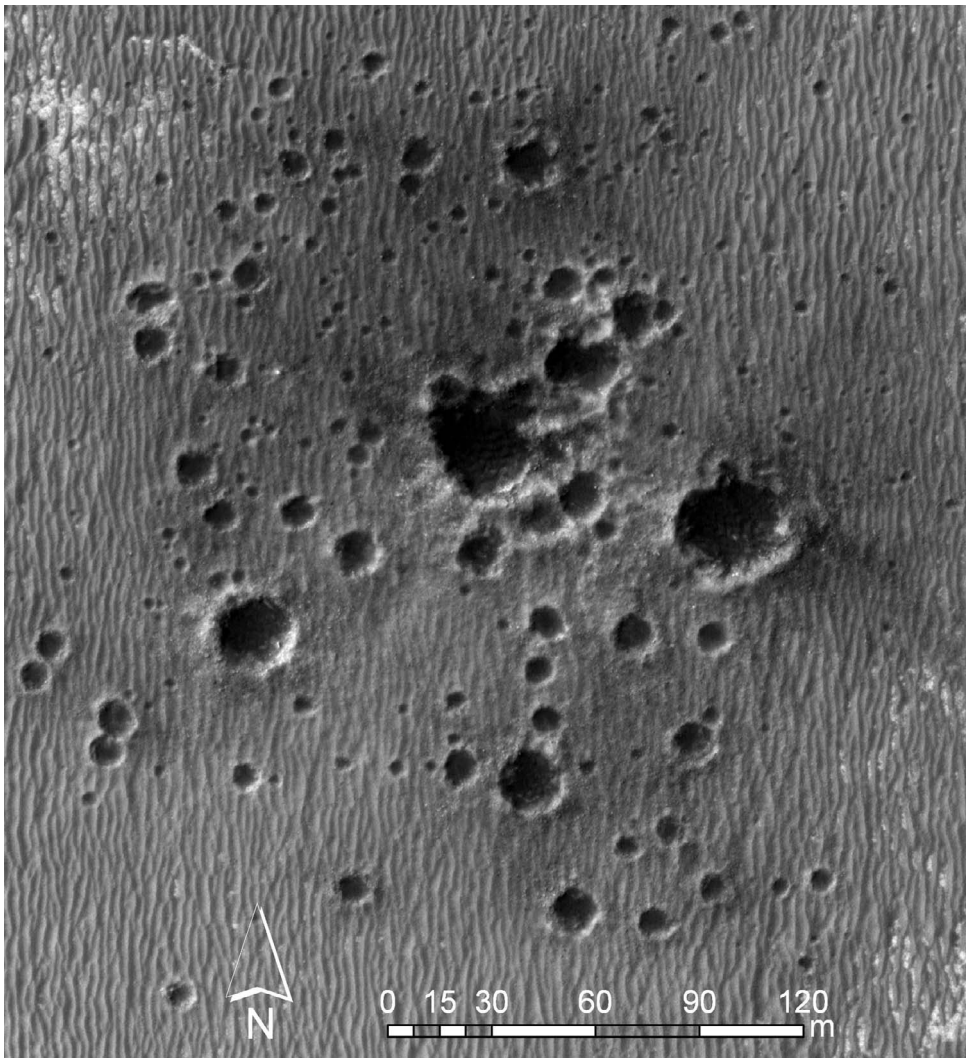

Figure 38. HiRISE image of relatively fresh crater cluster about 4 km west-northwest of Victoria crater in Meridiani Planum. The crater cluster is composed of >250 craters dispersed over several hundred meters, with the largest three craters 20–30 m in diameter, suggesting that it is a type 3 cluster produced by fragmentation by a low-density impactor (~1 g/cm^3) [*Ivanov et al.*, 2008]. Note eolian bed forms in the larger craters and how the north trending ripples overtake the rims of many of the craters. Portion of HiRISE image ESP_016644_1780.

landscape in the Late Amazonian has been extraordinarily slow [*Golombek et al.*, 2006a]. To estimate the rate of change that has occurred after an impact we take two examples. The first is the erosion and planing off of ejecta blocks around craters in the Kaikos cluster. Ejecta blocks around these craters have been eroded by saltating sand roughly parallel to the surface (Figure 37). Based on the size of these blocks, we estimate of order 10 cm of erosion has occurred since the impact roughly 200 ka. The second example is the erosion of a sulfate block near Concepción crater. This block has numerous blueberries eroding out of its surface (Figure 24) and accumulation of blueberries around its base. We calculated the amount of erosion of the block (30 cm diameter) necessary to erode 1–4 mm diameter blueberries with 1–4% volume density [*McLennan et al.*, 2005] that cover a several centimeter circumference around its base with packing densities of 0.9–0.7. Results suggest erosion of between 1 mm to 1 cm since the Concepción impact placed this block on the surface 1–10 ka. Both of these examples suggest erosion rates as rapid as of order 1 μ/yr, which is 2–3 orders of magnitude faster than long-term erosion rates calculated for the Amazonian at Meridiani Planum [*Golombek et al.*, 2006a]. Interestingly, erosion rates of order 1 μ/yr have been suggested for fine-layered deposits that are relatively free of craters [*McEwen et al.*, 2005] elsewhere on Mars. We interpret these results as follows. After an impact, ejecta with a wide variety of grain sizes including blocks are deposited on the surface out of equilibrium with the eolian regime. Sand size grains available are rapidly saltated by the wind, rapidly erode sulfate ejecta blocks in the wind stream, and are deposited in quiet areas around dense ejecta blocks and the crater interior. For

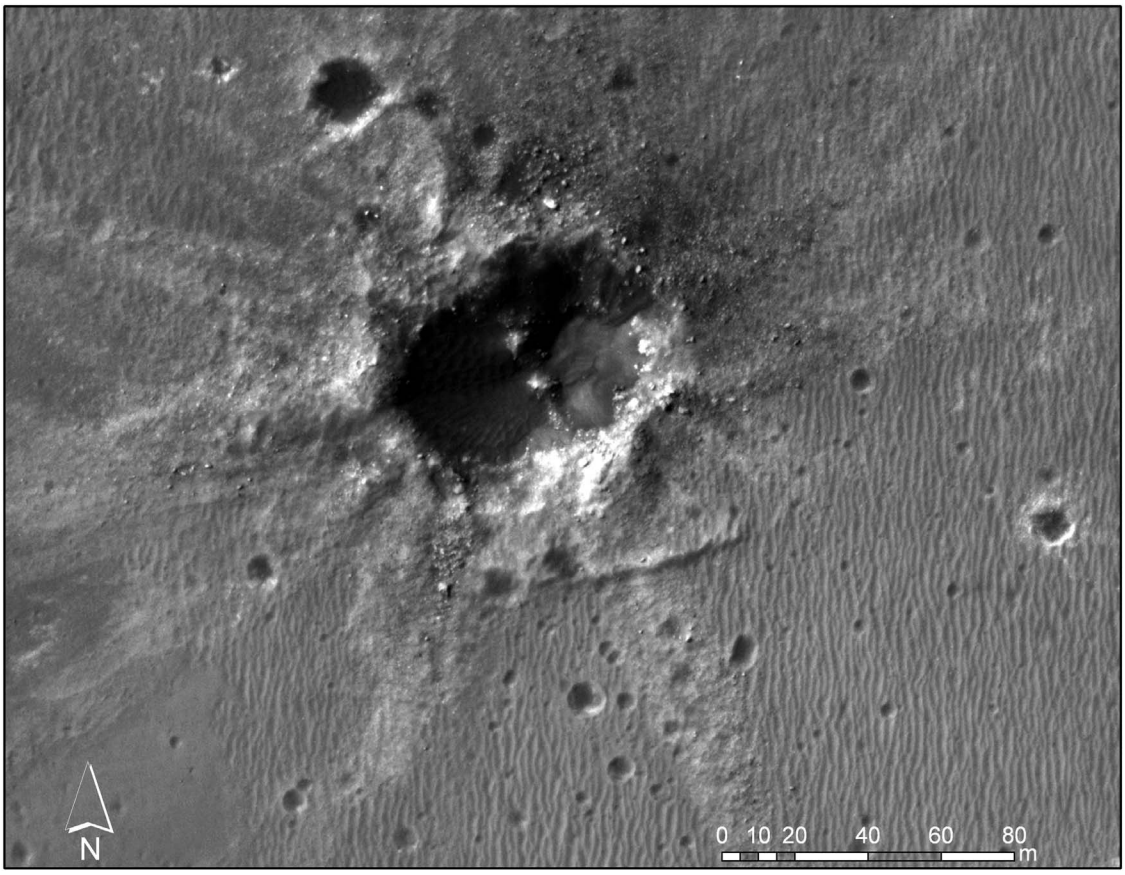

Figure 39. HiRISE image of relatively fresh doublet crater located about 15 km south-southwest of Victoria crater. Note eolian bed forms in the crater interior and north trending ripples that extend through the crater rays and heavily modify smaller companion crater rims. Note light-toned rays with smoothed topography, suggesting that the sulfate blocks have been planed off by eolian erosion. The presence of one large doublet crater with many smaller companion craters indicates this is a type 1 cluster formed by fragmentation of an impactor of density 1.8–3 g/cm^3 [*Ivanov et al.*, 2008]. Portion of HiRISE image ESP_016644_1780.

short periods, the rates of modification can be as high as 1 μ/yr, until the surface is brought back into equilibrium with the eolian regime. At that time, very little change occurs, yielding erosion rates that are 2–5 orders of magnitude lower over long time scales (of order billion years).

[61] If conditions were more favorable for ripple migration at Meridiani Planum (and perhaps elsewhere on Mars) prior to 50 ka, one possible cause could be differences in climate. Two important factors controlling the saltation of sand are near-surface winds and the density of the atmosphere. *Laskar et al.* [2002] has pointed out that large changes in insolation due to changes in obliquity and eccentricity occur at ~100,000 year intervals. Without a reservoir of CO_2 in the shallow crust (as yet unidentified), such insolation changes would not lead to a thicker atmosphere. If the atmosphere could not be thickened in the recent past from such a mechanism, then only increased wind speeds over such time scales could be evoked [e.g., *Haberle et al.*, 2003]. It remains to be seen if atmospheric models of Mars with obliquity and insolation changes over time scales of order 100,000 years predict higher wind speeds in the recent past, but our observations and the lack of evidence for significant dune migration suggests that atmospheric conditions were more favorable to saltating sand prior to 50 ka and less favorable since.

7. Summary and Conclusions

[62] Opportunity explored a cluster of very fresh craters about 2.3 km south of Victoria crater, called the Resolution crater cluster, that is composed of about 50 craters scattered across a 120 by 80 m area, of which the 4 largest craters are about 5 m in diameter. Opportunity observations of the Resolution crater cluster shows these craters are superposed on and thus younger than the north trending granule ripples of Meridiani Planum. The craters have uplifted rims, ejecta blocks perched on top of the granule ripples, with eolian modification limited to small secondary ripples. Dark, perched, centimeter size pebbles are strewn across the surface of these craters (as well as other craters), which are explained most simply if these pebbles are fragments of their respective impactors. The dispersion of the craters is similar to other clusters that have impacted in the past 10 years that form by fragmentation of weak or low-density impactors in the atmosphere. The craters are shallower than expected for fresh hypervelocity impacts, which could be due to lower cratering

efficiency expected for clustered impacts or due to atmospherically reduced impact velocities.

[63] Opportunity explored Concepción crater about 6 km south-southwest of Victoria crater, which is a 10 m diameter fresh crater with dark rays. Concepción crater is superposed on the ripples, and displays a fresh blocky interior wall, uplifted rim, and ejecta and rays that are superposed on the ripples. Concepción's rays are blocky ejecta of light-toned sulfate outcrop, indicating that shadows and shading from the ejecta blocks are responsible for their dark tone in the relatively low Sun angle HiRISE images. Color Pancam images show a dearth of blueberry hematite spheres perched on top of the surface adjacent to the crater or its ejecta, suggesting that they have been dispersed or buried by the impact and its ejecta.

[64] Two larger, fresh-rayed craters in Meridiani Planum imaged by HiRISE that impacted into surfaces with granule ripples similar to those traversed by Opportunity have extensive blocky rays (from their brightness in nighttime thermal images) and secondaries. Ada crater is a 2.2 km diameter crater, about 150 km east-southeast of Victoria crater, with secondaries about 6 km and 32 km to the south and south-southwest, respectively, that are clearly superposed on and thus younger than the north trending ripples. An unnamed 0.84 km diameter crater about 40 km west of Victoria crater has secondary craters about 9 km to the south that are heavily modified by ripples, with distorted noncircular shapes, dark sand filled interiors, and no obvious ejecta. These observations indicate that Ada crater formed after and the unnamed 0.84 km diameter crater formed before the latest phase of ripple migration at Meridinai Planum.

[65] Three largely independent methods are used to date the age of the latest phase of ripple migration at Meridiani Planum to between ~50 ka and ~200 ka. First, only craters younger than the ripples, with continuous, unbroken circular rims that truncate ripple crests, show no sign of eolian modification or bed forms inside or on the rims, and have ejecta blocks that are superposed on the ripples, were counted in a portion of a HiRISE image that includes part of Opportunity's traverse and the Resolution crater cluster. The size-frequency distribution of these craters defines a model age of ~50 ka, indicating that the latest phase of ripple migration occurred before then. Second, craters superposed on the continuous ejecta of Ada and the unnamed 0.84 km diameter craters with uplifted rims and fresh bowl shapes were counted and fall on the ~50 ka and ~200 ka model isochrons, respectively, suggesting that the latest phase of ripple migration occurred between ~50 ka and ~200 ka throughout Meridiani Planum. The third method estimates the recurrence intervals for the 32 freshest 0.5–5 km diameter rayed craters in the equatorial region of Mars, classified according to their relative age based on the amount of eolian modification, and their thermophysical properties. The calculated recurrence interval for Ada, the youngest 2.2–4 km crater of this size is ~400 ka, which is consistent with the ~50 ka age for Ada from the second method. The calculated recurrence interval for 0.84–4 km craters is ~30 ka, and because the unnamed 0.84 km diameter crater in Meridiani is the 5th–13th youngest crater of this size, it formed between ~120 ka and ~400 ka (or longer if the inventory of small rayed craters is incomplete), which is consistent with its ~200 ka age from the second method. Although the absolute model ages are highly uncertain, the relative age difference between the estimates is not.

[66] The hematite concentration measured by TES around Ada and the unnamed 0.84 km diameter crater is consistent with the estimated age of ripple migration. The strong TES hematite detection that was the main science factor that led to the selection of Meridiani Planum as a landing site for MER, is absent around the Ada crater in the same spatial pattern as the crater rays. Because the hematite signature is produced by blueberries (hematite concretions) that have weathered out of the sulfate outcrop and accumulated as a granule lag at the surface, and because Ada is younger than the latest phase of ripple migration, which produced their concentration at the surface, the lack of blueberries is consistent with their being mixed in the ejecta or perhaps dispersed by the impact generated air blast. In contrast, the hematite concentration around the unnamed 0.84 km diameter crater is reduced as would be expected if the crater impacted prior to the latest phase of ripple migration but the blueberries have been partially restored since.

[67] Observations of small craters at Meridiani and fresh-rayed craters elsewhere on Mars enable the development of a time scale for their formation based on their morphology, eolian modification, and preservation of rays. Craters that have impacted in the past decade appear very fresh, show no clear evidence for eolian modification and have fresh dark rays. A crater cluster in south Meridiani also appears very fresh without eolian modification, has bright yellowish and dark ray ejecta, and is estimated via recurrence intervals to have impacted several decades ago. Both the Resolution crater cluster and Concepción crater impacted after the latest phase of ripple migration or <50 ka. These craters have some eolian modification, with secondary ripples forming on the sandy rims of Resolution cluster craters, and sand deposited on the floor of Concepción crater and filled in among the ejecta blocks. The presence of dark rays around Concepción crater implies it is younger than Resolution, suggesting that Concepción impacted of order a thousand years ago and Resolution impacted a few tens of thousands of years ago. Ada impacted ~50 ka and has some eolian bed forms on its floor; Ada secondaries have dark centers (likely sand), bright rims, and are clearly superposed on the north trending ripples. Craters that formed before the latest phase of ripple migration have greater eolian modification and more distorted shapes (particularly small craters) from ripples that merge with and overtake their rims and sand-filled floors. Ejecta blocks around craters >200 ka have been eroded by saltating sand and many have been planed off or partially planed off parallel to the ripple surface. These craters also have sand deposited in their interiors and ripples that merge with and overtake their rims.

[68] The inactivity of the ripples over the past ~50 ka at Meridiani is consistent with the lack of observed eolian bed forms in craters that formed in the past 20 years, little evidence for the motion of dunes and other bed forms in the past 30 years, and the exceedingly low long-term erosion rates determined for the Amazonian and Late Amazonian at the landing sites. Interestingly, ~100 ka is the time scale for most recent obliquity variations and changes in insolation on Mars, which suggest that changes in climate (including

winds) could be responsible for the relative inactivity in eolian processes during the past ~100 ka.

[69] **Acknowledgments.** Research described in this paper was done by the MER and HiRISE projects, Jet Propulsion Laboratory, California Institute of Technology, under a contract with NASA. We thank E. Schaefer, E. Snead, E. Noe Dobrea, and J. Bell for help with the figures and J. Ashley, A. Vaughan, T. Parker, J. Grotzinger, J. Wray, M. Pendleton-Hoffer, R. Kienenberger, and an anonymous reviewer for comments.

References

Anderson, R. S. (1987), A theoretical model for aeolian impact ripples, *Sedimentology*, *34*, 943–956, doi:10.1111/j.1365-3091.1987.tb00814.x.

Anderson, R. S., and P. K. Haff (1988), Simulation of eolian saltation, *Science*, *241*, 820–823, doi:10.1126/science.241.4867.820.

Armstrong, J. C., C. B. Leovy, and T. Quinn (2004), A 1 Gyr climate model for Mars: New orbital statistics and the importance of seasonally resolved polar processes, *Icarus*, *171*, 255–271.

Arvidson, R., et al. (1979), Differential aeolian redistribution rates on Mars, *Nature*, *278*, 533–535, doi:10.1038/278533a0.

Arvidson, R. E., et al. (2003), Mantled and exhumed terrains in Terra Meridiani, Mars, *J. Geophys. Res.*, *108*(E12), 8073, doi:10.1029/2002JE001982.

Arvidson, R. E., et al. (2006), Nature and origin of the hematite-bearing plains of Terra Meridiani based on analyses of orbital and Mars Exploration rover data sets, *J. Geophys. Res.*, *111*, E12S08, doi:10.1029/2006JE002728.

Bagnold, R. A. (1941), *The Physics of Blown Sand and Desert Dunes*, Chapman and Hall, London.

Bourke, M. C., K. S. Edgett, and B. A. Cantor (2008), Recent aeolian dune change on Mars, *Geomorphology*, *94*, 247–255, doi:10.1016/j.geomorph.2007.05.012.

Christensen, P. R., et al. (2001a), Mars Global Surveyor Thermal Emission Spectrometer experiment: Investigation description and surface science results, *J. Geophys. Res.*, *106*, 23,823–23,871, doi:10.1029/2000JE001370.

Christensen, P. R., et al. (2001b), Global mapping of Martian hematite mineral deposits: Remnants of water-driven processes on early Mars, *J. Geophys. Res.*, *106*, 23,873–23,885, doi:10.1029/2000JE001415.

Christensen, P. R., et al. (2004), Mineralogy at Meridiani Planum from the Mini-TES experiment on the Opportunity rover, *Science*, *306*, 1733–1739, doi:10.1126/science.1104909.

Clark, B. C., et al. (2005), Chemistry and mineralogy of outcrops at Meridiani Planum, *Earth Planet. Sci. Lett.*, *240*, 73–94, doi:10.1016/j.epsl.2005.09.040.

Daubar, I., and A. McEwen (2009), Depth to diameter ratios of recent primary impact craters on Mars, *Lunar Planet. Sci.*, *XL*, Abstract 2419.

Daubar, I., et al. (2010), The current Martian cratering rate, *Lunar Planet. Sci.*, *XLI*, Abstract 1978.

Dundas, C. M., L. P. Keszthelyi, V. J. Bray, and A. S. McEwen (2010), Role of material properties in the cratering record of young platy-ridged lava on Mars, *Geophys. Res. Lett.*, *37*, L12203, doi:10.1029/2010GL042869.

Edgett, K. S. (2005), The sedimentary rocks of Sinus Meridiani: Five key observations from data acquired by the Mars Global Surveyor and Mars Odyssey orbiters, *Mars*, *1*, 5–58, doi:10.1555/mars.2005.0002.

Edgett, K. S., and M. C. Malin (2000), New views of Mars eolian activity, materials, and surface properties: Three vignettes from the Mars Global Surveyor Mars Orbiter Camera, *J. Geophys. Res.*, *105*, 1623–1650, doi:10.1029/1999JE001152.

Fenton, L. K. (2006), Dune migration and slip face advancement in the Rabe Crater dune field, Mars, *Geophys. Res. Lett.*, *33*, L20201, doi:10.1029/2006GL027133.

Fryberger, S. G., P. Hesp, and K. Hastings (1992), Aeolian granule ripple deposits, Namibia, *Sedimentology*, *39*, 319–331, doi:10.1111/j.1365-3091.1992.tb01041.x.

Gault, D. E., and J. A. Wedekind (1978), Experimental studies of oblique impact, *Proc. Lunar Planet. Sci. Conf.*, *9th*, 3843–3875.

Geissler, P. E., et al. (2008), First in situ investigation of a dark wind streak on Mars, *J. Geophys. Res.*, *113*, E12S31, doi:10.1029/2008JE003102.

Geissler, P. E., et al. (2010), Gone with the wind: Eolian erasure of the Mars rover tracks, *J. Geophys. Res.*, doi:10.1029/2010JE003674, in press.

Golombek, M. P., and N. T. Bridges (2000), Erosion rates on Mars and implications for climate change: Constraints from the Pathfinder landing site, *J. Geophys. Res.*, *105*, 1841–1853, doi:10.1029/1999JE001043.

Golombek, M. P., and R. J. Phillips (2010), Mars tectonics, in *Planetary Tectonics*, edited by T. R. Watters and R. A. Schultz, chap. 5, pp. 183–232, Cambridge Univ. Press, New York.

Golombek, M. P., et al. (2003), Selection of the Mars Exploration Rover landing sites, *J. Geophys. Res.*, *108*(E12), 8072, doi:10.1029/2003JE002074.

Golombek, M. P., et al. (2006a), Erosion rates at the Mars Exploration Rover landing sites and long-term climate change on Mars, *J. Geophys. Res.*, *111*, E12S10, doi:10.1029/2006JE002754.

Golombek, M. P., et al. (2006b), Geology of the Gusev cratered plains from the Spirit rover transverse, *J. Geophys. Res.*, *111*, E02S07, doi:10.1029/2005JE002503.

Grant, J. A., and T. J. Parker (2002), Drainage evolution of the Margaritifer Sinus region, Mars, *J. Geophys. Res.*, *107*(E9), 5066, doi:10.1029/2001JE001678.

Grant, J. A., et al. (2006), Crater gradation in Gusev crater and Meridiani Planum, Mars, *J. Geophys. Res.*, *111*, E02S08, doi:10.1029/2005JE002465.

Grant, J. A., et al. (2008), Degradation of Victoria crater, Mars, *J. Geophys. Res.*, *113*, E11010, doi:10.1029/2008JE003155.

Grotzinger, J. P., et al. (2005), Stratigraphy and sedimentology of a dry to wet eolian depositional system, Burns formation, Meridiani Planum, Mars, *Earth Planet. Sci. Lett.*, *240*, 11–72, doi:10.1016/j.epsl.2005.09.039.

Haberle, R. M., et al. (2003), Orbital change experiments with a Mars general circulation model, *Icarus*, *161*, 66–89, doi:10.1016/S0019-1035(02)00017-9.

Hartmann, W. (2005), Martian cratering 8: Isochron refinement and the chronology of Mars, *Icarus*, *174*, 294–320, doi:10.1016/j.icarus.2004.11.023.

Hartmann, W. K., and G. Neukum (2001), Cratering chronology and the evolution of Mars, *Space Sci. Rev.*, *96*, 165–194, doi:10.1023/A:1011945222010.

Hynek, B. M. (2004), Implications for hydrologic processes on Mars from extensive bedrock outcrops throughout Terra Meridiani, *Nature*, *431*, 156–159, doi:10.1038/nature02902.

Hynek, B. M., and R. J. Phillips (2001), Evidence for extensive denudation of the Martian highlands, *Geology*, *29*, 407–410, doi:10.1130/0091-7613(2001)029<0407:EFEDOT>2.0.CO;2.

Hynek, B. M., and R. J. Phillips (2008), The stratigraphy of Meridiani Planum, Mars, and implications for the layered deposits' origin, *Earth Planet. Sci. Lett.*, *274*(1–2), 214–220, doi:10.1016/j.epsl.2008.07.025.

Hynek, B. M., R. E. Arvidson, and R. J. Phillips (2002), Geologic setting and origin of Terra Meridiani hematite deposit on Mars, *J. Geophys. Res.*, *107*(E10), 5088, doi:10.1029/2002JE001891.

Ivanov, B. A. (2001), Mars/Moon cratering ratio estimates, *Space Sci. Rev.*, *96*, 87–104, doi:10.1023/A:1011941121102.

Ivanov, B., et al. (2008), Small impact crater clusters in high resolution HiRISE images, *Lunar Planet. Sci.*, *XXXIX*, Abstract 1221.

Ivanov, B., et al. (2009), Small impact crater clusters in high resolution HiRISE images - II, *Lunar Planet. Sci.*, *XL*, Abstract 1410.

Jerolmack, D. J., et al. (2006), Spatial grain size sorting in eolian ripples and estimation of wind conditions on planetary surfaces: Application to Meridiani Planum, Mars, *J. Geophys. Res.*, *111*, E12S02, doi:10.1029/2005JE002544.

Kreslavsky, M. (2009), Dynamic landscapes at high latitudes on Mars: Constraints from populations of small craters, *Lunar Planet. Sci.*, *XL*, Abstract 2311.

Lane, M. D., P. R. Christensen, and W. K. Hartmann (2003), Utilization of the THEMIS visible and infrared imaging data for crater population studies of the Meridiani Planum landing site, *Geophys. Res. Lett.*, *30*(14), 1770, doi:10.1029/2003GL017183.

Laskar, J., et al. (2002), Orbital forcing of the Martian polar layered deposits, *Nature*, *419*, 375–377, doi:10.1038/nature01066.

Laskar, J., A. C. M. Correia, M. Gastineau, F. Joutel, B. Levrard, and P. Robutel (2004), Long term evolution and chaotic diffusion of the insolation quantities of Mars, *Icarus*, *170*, 343–364.

Maki, J. N., et al. (2003), Mars Exploration Rover Engineering Cameras, *J. Geophys. Res.*, *108*(E12), 8071, doi:10.1029/2003JE002077.

Malin, M. C., and K. S. Edgett (2001), Mars Global Surveyor Mars Orbiter Camera: Interplanetary cruise through primary mission, *J. Geophys. Res.*, *106*, 23,429–23,570, doi:10.1029/2000JE001455.

Malin, M. C., et al. (2006), Present-day impact cratering rate and contemporary gully activity on Mars, *Science*, *314*, 1573–1577, doi:10.1126/science.1135156.

McEwen, A. S., et al. (2005), The rayed crater Zunil and interpretations of small impact craters on Mars, *Icarus*, *176*, 351–381, doi:10.1016/j.icarus.2005.02.009.

McLennan, S. M., et al. (2005), Provenance and diagenesis of the evaporite-bearing Burns formation, Meridiani Planum, Mars, *Earth Planet. Sci. Lett.*, *240*, 95–121, doi:10.1016/j.epsl.2005.09.041.

Mellon, M. T., et al. (2000), High-resolution thermal inertia mapping from the Mars Global Surveyor Thermal Emission Spectrometer, *Icarus*, *148*, 437–455, doi:10.1006/icar.2000.6503.

Melosh, H. J. (1989), Impact Cratering, 245 pp., Oxford Univ. Press, New York.

Mittlefehldt, D. W., et al. (2010), Marquette Island: A distinct mafic lithology discovered by Opportunity, *Lunar Planet. Sci.*, *XL*, Abstract 2109.

Parker, T. J., M. P. Golombek, and M. W. Powell (2010), Geomorphic/geologic mapping, localization, and traverse planning at the Opportunity landing site, Mars, *Lunar Planet. Sci.* [CD-ROM], *XLI*, Abstract 2638.

Phillips, R. J., et al. (2001), Ancient geodynamics and global-scale hydrology on Mars, *Science*, *291*, 2587–2591, doi:10.1126/science.1058701.

Pike, R. J. (1977), Size-dependence in the shape of fresh impact craters on the moon, in *Impact and Explosion Cratering*, edited by D. J. Roddy and R. B. Merrill, pp. 489–509, Elsevier, New York.

Pike, R. J., and D. E. Wilhelms (1978), Secondary-impact craters on the Moon: Topographic form and geologic process, *Proc. Lunar Planet. Sci. Conf.*, *9th*, 907–909.

Powell, M. W., T. M. Crockett, J. S. Norris, and K. S. Shams (2010), Geologic mapping in Mars Rover operations, paper presented at SpaceOps Conference, Am. Inst. of Aeronaut. and Astronaut., Huntsville, Ala., 25–30 Apr.

Putzig, N. E., et al. (2005), Global thermal inertia and surface properties of Mars from the MGS mapping mission, *Icarus*, *173*, 325–341, doi:10.1016/j.icarus.2004.08.017.

Quaide, W. L., and V. R. Oberbeck (1968), Thickness determination of the lunar surface layer from lunar impact craters, *J. Geophys. Res.*, *73*, 5247–5270, doi:10.1029/JB073i016p05247.

Schröder, C., et al. (2008), Meteorites on Mars observed with the Mars Exploration Rovers, *J. Geophys. Res.*, *113*, E06S22, doi:10.1029/2007JE002990.

Schultz, P. H., and D. E. Gault (1985), Clustered impacts: Experiments and implications, *J. Geophys. Res.*, *90*, 3701–3732, doi:10.1029/JB090iB05p03701.

Sharp, R. P. (1963), Wind ripples, *J. Geol.*, *71*, 617–636, doi:10.1086/626936.

Silvestro, S., L. K. Fenton, and D. A. Vaz (2010), Ripple migration and small modifications of active dark dunes in Nili Patera (Mars), *Lunar Planet. Sci.*, *XLI*, Abstract 1820.

Soderblom, L. A., et al. (2004), Soils of Eagle crater and Meridiani Planum at the Opportunity rover landing site, *Science*, *306*(5702), 1723–1726, doi:10.1126/science.1105127.

Squyres, S. W., et al. (2004a), In-Situ evidence for an ancient aqueous environment on Mars, *Science*, *306*, 1709–1714, doi:10.1126/science.1104559.

Squyres, S. W., et al. (2004b), The Opportunity rover's Athena science investigation at Meridiani Planum, Mars, *Science*, *306*, 1698–1703, doi:10.1126/science.1106171.

Sullivan, R., et al. (2005), Aeolian processes at the Mars Exploration Rover Meridiani Planum landing site, *Nature*, *436*, 58–61, doi:10.1038/nature03641.

Sullivan, R., et al. (2007) Aeolian geomorphology with MER Opportunity at Meridiani Planum, Mars, *Lunar Planet. Sci.*, *XXXVIII*, Abstract 2048.

Sullivan, R., et al. (2008), Wind-driven particle mobility on Mars: Insights from Mars Exploration Rover observations at "El Dorado" and surroundings at Gusev crater, *J. Geophys. Res.*, *113*, E06S07, doi:10.1029/2008JE003101.

Tornabene, L. L., et al. (2006), Identification of large (2–10 km) rayed craters on Mars in THEMIS thermal infrared images: Implications for possible Martian meteorite source regions, *J. Geophys. Res.*, *111*, E10006, doi:10.1029/2005JE002600.

Weitz, C. M., et al. (2006), Soil grain analyses at Meridiani Planum, Mars, *J. Geophys. Res.*, *111*, E12S04, doi:10.1029/2005JE002541.

Williams, K. K. (2006), Are Martian dunes migrating? A planet-wide search for dune movement, *Lunar Planet. Sci.*, *XXXVII*, Abstract 2322.

Williams, K. K., et al. (2003), Using overlapping MOC images to search for dune movement and to measure dune heights, *Lunar Planet. Sci.*, *XXXIV*, Abstract 1639.

Wiseman, S. M., et al. (2010), Spectral and stratigraphic mapping of hydrated sulfate and phyllosilicate-bearing deposits in northern Sinus Meridiani, Mars, *J. Geophys. Res.*, *115*, E00D18, doi:10.1029/2009JE003354.

Zimbelman, J. R. (2000), Non-active dunes in the Acheron Fossae region of Mars between the Viking and Mars Global Surveyor eras, *Geophys. Res. Lett.*, *27*, 1069–1072, doi:10.1029/1999GL008399.

Zimbelman, J. R., et al. (2009), The rate of granule ripple movement on Earth and Mars, *Icarus*, *203*, 71–76, doi:10.1016/j.icarus.2009.03.033.

N. Bridges, Johns Hopkins University Applied Physics Laboratory, Laurel, MD 20723, USA.

M. Golombek, Jet Propulsion Laboratory, California Institute of Technology, Pasadena, CA 91109, USA.

B. Ivanov, Institute for Dynamics of Geospheres, RAS, 119334, Moscow, Russia.

A. McEwen and L. Tornabene, Lunar and Planetary Laboratory, University of Arizona, Tucson, AZ 85721, USA.

K. Robinson, State University of New York at Binghamton, Binghamton, NY 13902, USA.

R. Sullivan, Department of Astronomy, Cornell University, Ithaca, NY 14853, USA.